Anisogamy Does Not Always Promote the Evolution of Mating Competition Traits in Males

Mattias Siljestam[1] **and Ivain Martinossi-Allibert**[2,*]

[1]Department of Ecology and Genetics, Animal Ecology, Uppsala University, Norbyvägen 18D, 752 36 Uppsala, Sweden

[2]Department of Biology, Norwegian University of Science and Technology NTNU, 7491 Trondheim, Norway

ORCIDs: Siljestam, https://orcid.org/0000-0002-3720-4926; Martinossi-Allibert, https://orcid.org/0000-0002-8332-8620

ABSTRACT: Anisogamy has evolved in most sexually reproducing multicellular organisms allowing the definition of the male and female sexes, producing small and large gametes. Anisogamy, as the initial sexual dimorphism, is a good starting point to understand the evolution of further sexual dimorphisms. For instance, it is generally accepted that anisogamy sets the stage for more intense mating competition in males than in females. We argue that this idea stems from a restrictive assumption on the conditions under which anisogamy evolved in the first place: the absence of sperm limitation (assuming that all female gametes are fertilized). Here, we relax this assumption and present a model that considers the coevolution of gamete size with a mating competition trait, starting in a population without dimorphism. We vary gamete density to produce different scenarios of gamete limitation. We show that, while at high gamete density the evolution of anisogamy always results in male investment in competition, gamete limitation at intermediate gamete densities allows for either females or males to invest more into mating competition. Our results thus suggest that anisogamy does not always promote mating competition among males. The conditions under which anisogamy evolves matter, as well as the competition trait.

anisogamy | mating competition | gamete motility | gamete limitation | adaptive dynamics | sexual selection

Introduction

Anisogamy is widespread among sexually reproducing multicellular organisms (Lessells et al., 2009), across animals, plants, and fungi. Because it is the earliest possible sexual dimorphism to have evolved, anisogamy is likely to have influenced the evolution of later sexual dimorphisms or sex-biases by affecting how the sexes experience selection on reproductive traits. Here, we focus on the relationship that anisogamy bears with the evolution of sex-biases in traits involved in intrasexual competition for mating opportunities, a question that belongs to the field of sexual selection. The sexual selection perspective has so far been centred on the study of animal species, and with a bias towards clades that exhibit conspicuous morphologies and behaviours related to sexual selection (Beekman et al., 2016). Such a bias could restrict our understanding of the evolutionary dynamics at play, by generalizing from the special cases of motile organisms, that are internal fertilizers or targeted external fertilizers and may not represent well the ancestral species in which the transitions from isogamy to anisogamy would have occurred (Parker, 2014).

Here, we attempt to clarify the relationship between the evolution of anisogamy and sex-biases in mating competition traits, by taking the point of view of sessile broadcast spawning animals transitioning from isogamy to anisogamy. In the introduction, we explore the current line of thinking about the relationship between anisogamy and sex-biases in competition for matings in

Conceptualization: I.M.; Methodology: M.S.; Model analysis: M.S.; Data visualization: M.S.; Writing: I.M and M.S.; Funding Acquisition: I.M.

Authors declare no competing interests.

*To whom correspondence should be addressed. E-mail: imartinossi@gmail.com

the field of sexual selection, largely dominated by the Darwin-Bateman paradigm (Dewsbury, 2005) stating that anisogamy should generally favour more intense competition for mating in males. We highlight what we consider to be hidden restrictive assumptions that underlay this claim. We propose predictions regarding the evolution of sex-biases in mating competition traits corresponding to different scenarios of anisogamy evolution: they include, but are not limited to, the predictions made by the Darwin-Bateman paradigm. We then present and analyse an evolutionary dynamics model of the coevolution of gamete size and mating competition traits, starting in an isogamous population.

Anisogamy and the Darwin-Bateman paradigm. The field of sexual selection strives to describe patterns of sex-differences in competition for mating and understand their evolutionary origin (Andersson, 1994, pages 5-7). An empirical approach to the question suggests that, in the range of species studied today from the perspective of sexual selection, competition for mating is on average more intense in males (Janicke et al., 2016; Singh and Punzalan, 2018), although there is large inter- and intraspecific variation, sometimes within populations and on short time scales (e.g. Forsgren et al., 2004). This general trend raises the possibility that anisogamy could ultimately be favouring the evolution of traits involved in competition for mating in the sex with the smaller, more numerous gametes. Nevertheless, a well-supported underlying mechanism is missing to conclude to a causal link with anisogamy. In addition, most species for which this type of sex-specific data are available (see Janicke et al., 2016) are model organisms or have been the focus of sexual selection studies because they present conspicuous mating traits and thus do not represent a random sample of taxa.

The so-called "Darwin-Bateman" paradigm (Dewsbury, 2005) proposes that males should often experience stronger selective pressure to invest in mating competition traits because anisogamy causes variance in reproductive success to be higher in males than in females, a pattern directly caused by differences in gamete numbers. Another way to understand the argument is that female reproductive success is limited by fecundity, because all female gametes are always fertilized, sperm being in excess, while male reproductive success is limited by the number of mates. This line of thinking originated with the verbal arguments of Bateman (1948), which were influential in the field of sexual selection and fruitfully criticized (see Sutherland, 1985; Tang-Martinez and Ryder, 2005; Gowaty et al., 2012; Hoquet, 2020), leading to several controversies on the actual evolutionary forces at play (e.g. Queller, 1997; Kokko and Jennions, 2008; Fromhage and Jennions, 2016). The Darwin-Bateman paradigm is currently widely accepted in the field of sexual selection (Schärer et al., 2012; Janicke et al., 2016; Parker and Pizzari, 2015; Parker, 2014; Lehtonen et al., 2016; Fromhage and Jennions, 2016, to cite a few). However, it relies on the assumption that sperm limitation is absent, a view that may have been influenced by model species chosen for the study of sexual selection.

Thinking like a sessile broadcast spawner. To avoid being influenced by analogies with classical sexual selection model systems (birds, fish, amphibians, or insects) that have evolved in an anisogamous state for a long time, let us instead imagine a scenario involving animals that resemble the ones that are likely to have transitioned from isogamy to anisogamy in the first place: sessile marine broadcast spawners (Lehtonen and Parker, 2014; Parker, 2014). Being external fertilizers, they release gametes in the water column and there is no direct contact between mating partners or between parents and offspring. This precludes post-fertilization parental care, but does not prevent sexual selection from acting through competition and mate choice. Indeed, as is the case for all sessile sexually reproducing species (Beekman et al., 2016), broadcast spawners can develop gamete-level traits that allow competition or mate choice to occur as gametes encounter before fertilization (Evans and Sherman, 2013;

Kekäläinen and Evans, 2018). It is important to realize that these gamete-level traits influence the reproductive success of adult individuals and are thus comparable to classical examples of sexually selected traits (e.g. peacock tail or deer antlers). Because of external fertilization, broadcast spawners can also easily be subjected to situations of gamete limitation, where the assumption that sperm is in excess does not hold (Levitan and Petersen, 1995; Levitan, 1998*a*,*b*; Yund, 2000; Crean and Marshall, 2008). Given that sessile marine broadcast spawners are expected to be the ancestral stage transitioning from isogamy to anisogamy (Lehtonen and Parker, 2014; Parker, 2014), this raises the question of the role of gamete limitation in the evolution of anisogamy.

Anisogamy, from gamete competition to gamete limitation. Classically, there are two main theoretical frameworks for the evolution of anisogamy in animals (Lehtonen and Parker, 2014), *gamete competition* and *gamete limitation*. *Gamete competition* refers to a context where gamete encounters are frequent so that competition between the more numerous male gametes is the limiting factor for their fertilization success, while *Gamete limitation* refers to a context where gamete encounter rate is so low that it becomes the limiting factor for fertilization success of both sexes.

In the *gamete competition* framework, initially developed by Parker (Parker et al., 1972), the evolution of anisogamy is mainly driven by a constraint imposed on the survival of the zygote (Bulmer and Parker, 2002), which itself depends on gamete size: larger gametes harbour more resources and provide zygotes with higher survival chances. In this framework, there is no sperm limitation because gamete density is high enough and gametes encounter each other easily, which means that all larger gametes are automatically fertilized while some proportion of the smaller gametes are in excess. In the *gamete limitation* framework, which originated with Kalmus (Kalmus, 1932) the evolution of anisogamy arises as a strategy to increase gamete encounter rates, in an environment where gamete density is very low (see also Dusenbery, 2000; Iyer and Roughgarden, 2008). The evolution of anisogamy in this framework is favoured by gamete limitation, i.e. the fact that not all the gametes get fertilized and this suggests that both sexes could experience selection to develop traits increasing fertilization success. Thus, in the classical *gamete competition* framework, we find the conditions for females to evolve as a provisioning parent and males as intrasexual competitors, which is concordant with the Darwin-Bateman paradigm, while in the *gamete limitation* framework both sexes have the scope to invest into a competition trait that could increase their fertilization success, given that not all female eggs are fertilized.

Lehtonen and Kokko (2011) showed that *gamete competition* and *gamete limitation* are not two mutually exclusive theories on the evolution of anisogamy, but rather two complementary ideas that speculate on how anisogamy may have evolved in populations of high or low gamete densities. Gamete densities can vary continuously, and we envision the classical scenarios of *gamete competition* and *gamete limitation* as opposite extremes on that spectrum. The complete absence of gamete limitation corresponding to the classical *gamete competition* scenario would be a special case, occurring only at very high gamete density. As gamete density decreases, gamete limitation would appear but would not preclude competition for mating. As competition intensity decrease with decreasing gamete density, it can eventually become negligible at the lower extreme of the spectrum, which corresponds to the classical *gamete limitation* scenario and is termed here extreme gamete limitation.

Given the putative role of broadcast spawners in anisogamy evolution and them being subjected to sperm limitation in contemporary species, the role of gamete limitation in the evolution of anisogamy and competition for mating should be investigated. In recent years, researchers have generally emphasized the importance of sperm limitation in fully understanding

sexual selection (Iyer and Roughgarden, 2008; Levitan, 1998*b*; Beekman et al., 2016; Evans and Sherman, 2013) and the evolution of anisogamy (Dusenbery, 2000, 2006; Lehtonen and Kokko, 2011). We now want to understand how it can influence the connection between anisogamy and traits involved in competition for mating.

Does anisogamy promote male competition? The Darwin-Bateman paradigm assumes that anisogamy causes males to compete because their gametes are always in excess. However, models of the evolution of anisogamy do not imply the absence of sperm limitation, and contemporary broadcast spawning species are often subject to gamete limitation. We thus feel that there is a disconnect between theories of the evolution of anisogamy, and how the role of anisogamy is integrated in theories of the evolution of sex-biases in competition for mating. In particular, the consequences of gamete limitation on the evolution of sex-specific competition for mating remain largely unexplored (but see Lehtonen et al., 2016). We want to bridge this gap with a model that explores the role that anisogamy, as a first sexual dimorphism, can have in the evolution of sex-biases in mating competition traits. To do this, we start from a population with two mating types but no sexual dimorphism, and allow both gamete size and a competition trait to coevolve, drawing from the same fixed energy budget allocated to reproduction.

We predict in agreement with previous work (Schärer et al., 2012; Lehtonen et al., 2016) that in a model of the evolution of anisogamy in the absence of gamete limitation, mating competition traits should evolve more readily in males, as this situation already presupposes male competition and the absence of female reproductive failure. However, we argue that with some degree of gamete limitation either sex should be able to evolve competition traits, due to the fact that both could maximize their reproductive success that way. The final outcome could be dependent on the sex-specific cost of the competition trait (Kokko et al., 2012).

In the following sections, we develop and analyse a mathematical model of the coevolution of gamete size together with a mating trait starting in a population without sexual dimorphism. The mating traits affect fertilization success and we consider them to be competition trait whenever they impose a cost on the reproductive success of other individuals of the same mating type (intrasexual cost). We consider a population of sessile marine invertebrates releasing gametes in the water column, and, inspired by Lehtonen and Kokko (2011), we vary population density continuously to explore increasing levels of gamete limitation. Individuals have a fixed energy budget that can be allocated to either gamete provisioning (gamete size) or mating traits. Gamete and zygote survival probability are a function of their size. Fertilization events are controlled by a time-dependent process that accounts for gamete density, size and speed, and is Fisher consistent (the total number of male and female fertilizations are equal). We analyse independently the evolution of two types of mating traits, of which the effect on fertilization success is mechanistically described in the model. They are typical mating competition traits for sessile organisms (Beekman et al., 2016): gamete-level traits that allow adults of the same mating type to compete with each other over fertilization opportunities. The first type is gamete motility traits, often found in nature prominently in the smaller gametes. The second type is traits increasing the apparent size of the gametes, which boosts the ability to capture nearby gametes of the opposite mating type, corresponding to several strategies observed in nature: chemoattraction and jelly coat surrounding the larger gametes of several marine invertebrates (e.g. Farley and Levitan, 2001; Podolsky, 2002). We focus on parameter spaces where mating competition occurs and explore several possible relationships between gamete size and cost efficiency of the mating traits based on mechanistic modelling. We then examine the resulting evolving sex-bias in energy investment to the mating competition trait.

Model

We present a mechanistic mathematical model of the evolution of anisogamy, where we consider the coevolution of gamete size (volume) and a mating trait in a population of sessile marine animals with two mating types, reproducing through external fertilization. We first give a verbal and graphical presentation of the structure and analysis of the model before going into the mathematical details.

The life cycle of the organism is modelled in two steps and assumes discrete, non-overlapping generations (Figure 1). In the first step of the life cycle, a fixed number of brooding spots on the sea floor are occupied by adult individuals that produce gametes. Individuals share the allocation of a fixed reproductive budget between the production of gamete and investment into a mating trait. The mating trait increases the gamete fertilization success of individuals, but is at the exclusion of another fitness component, as it reduces the number of gametes produced per individual due to the investment trade-off. The mating

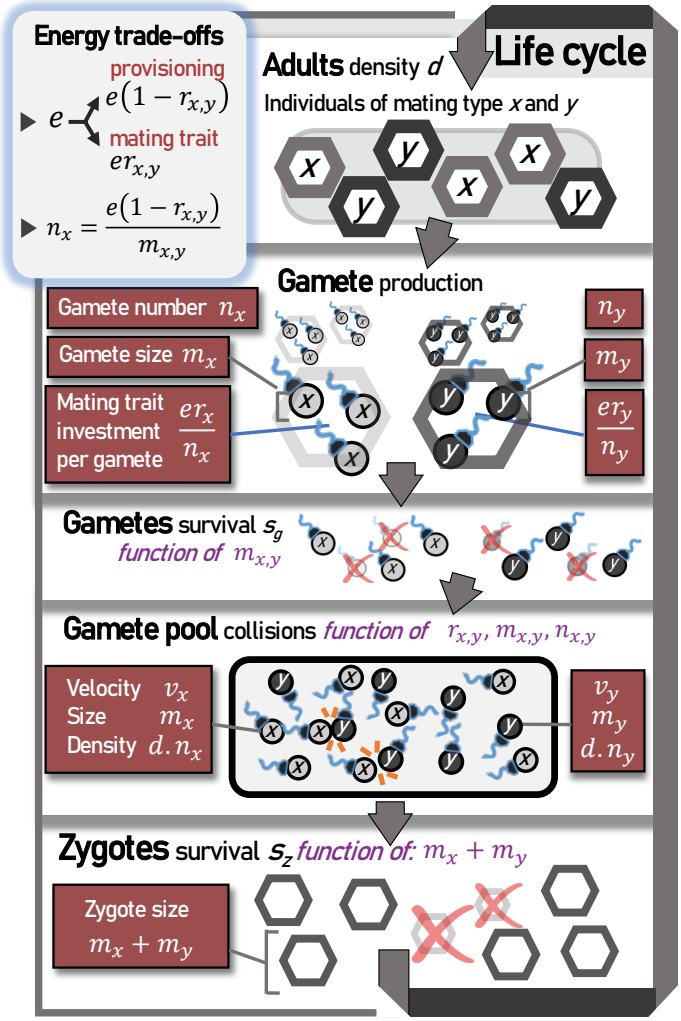

Fig. 1. Diagram representation of the model structure, with the complete life cycle and main parameters. The different trade-offs of energy allocated to reproduction are represented in the top left panel, where e is the fixed total energy budget allocated to reproduction by each individual. e can be invested into provisioning (gamete mass) which increases gamete and zygote survival, or into a mating trait increasing fertilization success. $r_{x,y}$ and $m_{x,y}$, respectively, the relative investment in mating trait and gamete mass are the two coevolving traits, independent for the x and y mating types. Hexagons represent diploid individuals, either adults with a determined mating type (x or y) or newly formed zygotes prior to mating type determination. Circles represent haploid gametes, marked with the mating type of the parent individual and only able to fertilise gametes marked with the opposing mating type. Red crosses denote gametes or zygotes that do not pass the size-dependent survival stages.

trait affects the reproductive success of other individuals in the population as well. It can impose a cost to other individuals of the same mating type (intrasexual cost of the trait), in which case the mating trait is termed a mating competition trait. At the same time, the mating trait is likely to increase the reproductive success of individuals of the other mating type (intersexual benefit of the trait) in most scenarios where gamete density is not extremely high. Intrasexual cost and intersexual benefit are not mutually exclusive. We quantify the intrasexual cost of the mating trait and use it to define parameter spaces of interest, where substantial competition for mating occurs. The number of gametes is also traded off against the size of each gamete, with larger gametes having a higher chance of surviving to the next step of the life cycle (Figure 2). Although there is little empirical data on the specific relationship between gamete size and survival (but see: Togashi et al., 1997), it seems reasonable to assume that larger gametes are more robust and thus have greater chances to survive to enter the mating pool.

In the second step of the life cycle, gametes are synchronously released into a common mating pool. In this mating pool, the gametes have a fixed amount of time during which they have to find a fusion partner to fertilize. Fertilizations occur as the result of collisions between gametes of opposite mating types, generating zygotes, the volume of which corresponds to the added volumes of the gametes (Figure 1). Zygote survival is also size-dependent (Figure 2). Surviving zygotes enter the next generation as adult individuals. Our model does not make restrictive assumption on the genetic architecture of the sex determination system. However, it does assume that individuals are produced in equal frequencies for both mating types.

In our analysis, we investigate the evolution of anisogamy by allowing for coevolution of two gametic traits: gamete size and the relative investment into the mating trait. We assume evolution to start under the constraint of isogamy, meaning equal trait values for both mating types. Under the isogamic constraint, the gamete traits of the population evolve towards an isogamic attractor. If asymmetric selection appears, such as disruptive selection, the constraint can then be removed, which would correspond to the evolution of a genetic machinery allowing for sexual differentiation, and anisogamy evolves. Even though disruptive selection can appear already before reaching the isogamic attractor, we assume that evolving the genetic machinery necessary to remove the isogamic constraint is non-trivial, so that the system reaches the attractor before the constraint is removed. Therefore, we first solve for evolutionary attractors under constrained isogamy. Then, we determine if these isogamic attractors are endpoints of evolution or if disruptive selection appears, leading to the evolution of anisogamy. For parameter combinations where anisogamy arises, we determine how the trait values of gamete size and investment in the mating trait evolve for the two mating types by solving for the evolutionary path.

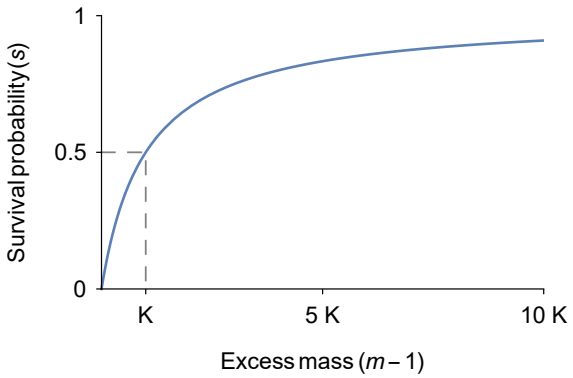

Fig. 2. Survival probability of gametes and zygotes as a function of their excess mass (volume) allocated to survival, $m - 1$. A survival of 50% is reached when the excess mass equals the half-saturation constant K marked out by the dashed line.

Gamete production. In the first step of the life cycle, surviving adult individuals are randomly chosen to occupy brooding spots occurring with a density of $2d$, where they can produce gametes. Surviving individuals are assumed to be in abundance such that all brooding spots are occupied. As the two mating types x and y are in equal frequency, individuals of each mating type occupy spots with a density of d. Each individual possesses a fixed amount of energy e allocated to gamete production. A proportion of the energy r_i is spent on a mating trait (see details further down), where i denotes the mating type and can be either x or y. We refer to the trait r_i as relative mating trait investment (or shortly, mating trait investment). The remaining energy $e(1-r_i)$ is converted into gamete volume, with each gamete having a volume of m_i. The number of gametes n_i produced per individual of mating type i is thereby a function of both the gamete volume m_i and the mating trait investment r_i, and is given by

$$n_i(m_i, r_i) = \frac{e(1-r_i)}{m_i}, \qquad [1]$$

where one can see that the investment into the mating trait r_i is traded off against gamete numbers n_i, as mentioned above.

The probability that a gamete survives until it enters the mating pool (the second step of the life cycle) is an increasing function of its size. We assume gamete cells must have a minimum volume of $m_i = 1$ to perform their function and that any additional gamete size, $m_i - 1$, makes the gamete more robust and therefore more likely to survive. The survival probability of a gamete s_g is given by the following saturating function $s_g(m_i) = (m_i - 1)/(K_g + m_i - 1)$, where K_g gives the half-saturation constant of gamete survival, i.e. the excess mass required for a 50% probability of survival (Figure 2). We will refer to K_g as the gamete size-survival parameter, where the survival probability drops quickly for gametes with sizes smaller than K_g.

Hence, the number of gametes entering the mating pool, per individual of mating type i, $n_{i,0}$, equals the number of gametes produced times their survival probability: $n_{i,0}(m_i, r_i) = n_i(m_i, r_i)s_g(m_i)$.

Note, the gamete survival function is qualitatively similar to the one used in Bulmer and Parker (2002), but ours only has one parameter. In contrast to Bulmer and Parker (2002), where the survival function models both the gamete survival and gamete fertilization probability, our survival function only gives initial gamete survival. We model the gamete fertilization dynamics mechanistically as presented below.

Gamete fertilization. In the mating pool, the second and last step of the life cycle, gamete fertilization occurs, which produces the zygotes that will become the adult individuals of the next generation. Here, the gametes that survived enter the mating pool, with a fixed amount of time t_{end} after which the mating period ends. During the mating period, the gametes move around randomly and can collide with each other. Each collision between gametes of the two mating types x and y results in a fertilization with probability p. A fertilization event removes both gametes from the mating pool and produces a zygote. To determine the collision frequency between gametes of the two mating types, we use collision theory (originally used to model chemical reaction rates between gas particles, McNaught et al., 2014). The collision frequency depends on three factors: the sizes of the gametes m_x and m_y, the gamete speeds v_x and v_y (see details further down) and the density of gametes, where all three factors increases the collision frequency (see Appendix A1, Eq. A1).

The initial gamete density of mating type i is given by $n_{i,0}(m_i, r_i)d$, i.e. the number of surviving gametes per individual contributing to the mating pool (at $t = 0$) multiplied by the population density d. The number of gametes then declines over time as they collide and get fertilized. At the end of the mating time t_{end}, the fertilization success f_i is given by the fraction of fertilized gametes $f_i = (n_{i,0} - n_{i,t_{\text{end}}})/n_{i,0}$ forming zygote offspring (Figure 3, Eq. A6). Higher population density increases

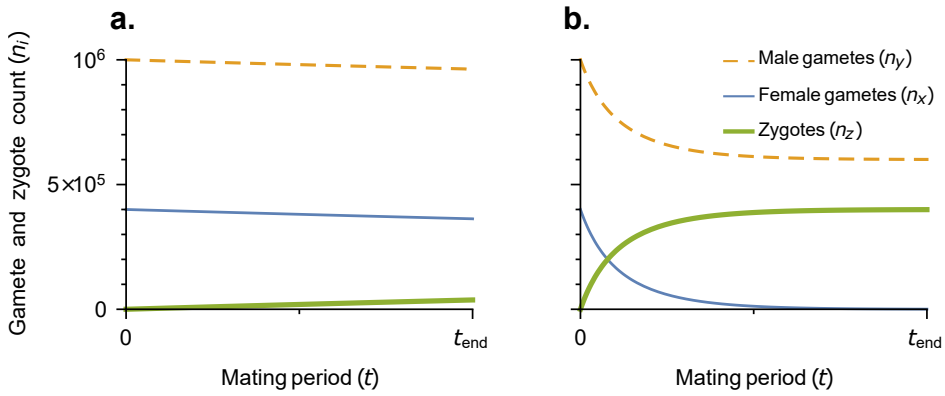

Fig. 3. Number of gametes and zygote offspring per adult individual over the mating period under **a.** *gamete limitation* (low gamete density) and **b.** *gamete competition* (high gamete density). These graphs are given by equation A6 with parameters: initial female gamete count $n_{x,0} = 5 \times 10^5$, initial male gamete count $n_{y,0} = 10^6$ and the product of $pd\sigma_{xy}v_{xy}$ equals 10^{-7} in **a.** and 10^{-5} in **b.** (this product contains population density d and is proportional to the gamete fertilization rate)

the chances for the gametes to find a fusion partner within the mating time (compare low and high population density in Figure 3**a** and **b**, respectively).

The life-cycle completes by the zygotes having to survive until adulthood. Just as for the gametes, the survival probability of zygotes is an increasing function of volume m_z (which is given by the combined volumes of the two gametes that fused to produce it $m_z = m_x + m_y$) according to $s_z(m_x, m_y) = (m_x + m_y - 1)/(K_z + m_x + m_y - 1)$, where K_z gives the half-saturation constant of zygote survival (Figure 2), and we will refer to K_z as the zygote size-survival parameter.

The mating traits and mating competition. We define a mating trait as a trait increasing the fertilization success f_i. The trait is subjected to an evolutionary trade-off, whereby investing into the mating trait is at the cost of reducing another fitness component (in our model, gamete numbers in Eq. 1, we elaborate more on this in Supplementary information S2.4). We investigate separately two alternative types of mating traits: gamete motility or fusion partner capture, and we are particularly interested in parameter spaces where these traits are involved in competition for mating. We quantify competition by the intrasexual cost of the trait, which is defined as the reduction in the reproductive success of a focal individual caused by an increased investment in the mating trait in individuals of the same mating type (see Supplementary information S2.6). For example, an intrasexual cost of 1 means that the mating trait causes a reduction in relative fitness of the focal individual equal to the increase in proportional investment (without trade-off) into the mating trait of individuals of the same mating type. Accordingly, an intrasexual cost of 0.1 means that the reduction in relative fitness of the focal individual is one tenth of the increase in proportional investment into the mating trait. In a similar way, we define the intersexual benefit of the mating trait as the increase in fitness perceived by a focal individual when the mating trait of the other mating type increases. We note that the intrasexual cost and intersexual benefit of the mating trait do not describe selection on the trait, or explain why the trait evolves, but rather describe population level consequences of the evolution of the trait.

(i) Competition through motility: In this scenario, we assume that gametes are in still water, resulting in no basal motility of the gametes. The mating trait is then a flagella-like mobility structure that allows gametes to move and encounter a fusion partner.

To mathematically derive the gamete speed, we use fluid mechanics assuming spherical gametes and rely on the two different methods proposed by Dusenbery (2009), giving different outcomes in terms of the size-speed relationships (see Supplementary information S1.1 for full details and derivations). The first method is strictly mechanistic, and we assume that (i) the metabolism dedicated to propulsion is proportional to the energy spent on the propulsion trait and (ii) the thrust of the propulsion trait is proportional to the metabolism dedicated to it. Applying fluid dynamics principles for friction of small entities in water (small Reynolds numbers), this scenario results in gamete speed being proportional to linear size (radius). There is good empirical evidence for such a linear size-speed relationship when comparing the motility of small organisms in water across a large range of genera of different sizes (Dusenbery, 2009, Fig. 8.3), as well as comparing gamete speeds between different genera (Dusenbery, 2009, Table 20.1).

The second method has a less mechanistic underpinning, but is based on insights from empirical evidence comparing gamete speeds within genera. In that case, data suggests that it may be more appropriate to assume the force of propulsion to be invariant to cell size (Dusenbery, 2009, Table 20.1). This assumption leads to gamete speed being inversely proportional to the radius, which is the classically assumed scenario for earlier mechanistic models of anisogamy evolution (Hoekstra, 1984; Hoekstra et al., 1984; Dusenbery, 2000, 2006; Togashi et al., 2009).

These two approaches result in opposite behaviour in terms of the size-speed relationships, but both relationships have empirical support at different scales. This leaves us with two different size-speed relationships that are relevant to consider, and we find that both can be expressed by the following equation,

$$v_i(m_i, r_i) = v_0 \sqrt{\frac{r_i}{1 - r_i}} m_i^{\alpha_m/3}, \qquad [2]$$

where v_0 is a velocity scale factor and α_m determines how gamete speed is affected by gamete size m_i. The positive size-speed relationship is given by $\alpha_m = 1$ and the negative size-speed relationship by $\alpha_m = -1$. An intermediate value of α_m corresponds to an intermediate scenario where for $\alpha_m > 0$, larger gametes are faster than smaller gametes for a given proportional investment r_i, while $\alpha_m < 0$ results in smaller gametes being faster for the same r_i.

(ii) Competition through fusion partner capture: In this scenario, we assume that all gametes are in suspension in water currents, and have similar motility due to the movement of their environment with gamete speed given by just the basal velocity v_0.

Here, we introduce another type of mating trait, which increases the collision target size of the gamete. Gametes move around randomly, with similar motility v_0, which is invariant to size, and the mating trait either increases the gamete target size through physical structures or by chemoattraction. In the absence of this trait, the gamete volume m is made of the expensive vital structures, increasing the survival probability of both the gamete and its potential zygote. The mating trait introduces a less costly way of increasing the collision target, but without giving any benefits in terms of survival of the gamete or zygote. The efficiency of this trait depends on α_d, the dimensionality of the scaling between energy invested and increase in apparent volume (see Supplementary information S1.2 for full details and derivations).

We consider several variants of the trait's physical structure, where different limiting or costly cellular compounds lead to different dimensionalities of the cost. First, we consider that the compound used to fill the apparent volume is costly (although cheaper than the regular cell volume). This fits the biological scenario of producing a jelly coat outside the cell membrane

or adding cytoplasm. The cost of the trait is then relatively high because it is proportional to the increased volume, and its dimensionality is therefore $\alpha_d = 3$. Second, we consider that the cost of increased volume mostly comes from compounds of the cell membrane, which gives a cost proportional to increased surface area, with a dimensionality $\alpha_d = 2$. For completeness, we include a third variation of this competition trait, for which we lack a good biological example. In this third scenario, the main cost comes from a cellular function that scales with the radius of the cell, and its dimensionality is therefore $\alpha_d = 1$.

The following single equation gives the volume of the collision target of a gamete of mating type i,

$$\hat{m}_i(m_i, r_i) = m_i \left(1 + 10 m_i^{(3-\alpha_d)/3} \frac{r_i}{1 - r_i}\right)^{3/\alpha_d}. \quad [3]$$

where α_d gives the dimensionality at which the mating trait scales with energy investment, and a value of 3, 2 or 1 corresponds to producing jelly coat, membrane area and a function with a cost scaling with cell radius, respectively.

As an alternative to the scenarios above, where the gamete uses physical structures to increase its collision target, we also consider a scenario where gametes can use chemoattraction to attract a fusion partner. In this case, the gametes produce and release chemoattractants and can be detected at a certain threshold concentration. At detection, which is always caused by the gamete with the larger chemoattractant zone, fertilization ensues. A particularity of chemoattraction is that the trait is only effective in the mating type with the larger chemoattraction radius, because the chemoattractant from the mating type with the smaller radius will never reach the cell surface of the other mating type before detection occurs in the other direction. The chemoattractant therefore increases the apparent volume of the collision-target of the gamete with the larger chemoattractant zone, which is given by Eq. 3 with $\alpha_d = 1$, and the volume simply remains $\hat{m}_j(m_j) = m_j$ for the mating type with the smaller chemoattractant zone (i.e., the mating trait investment r_j has no effect).

Analysis

We investigate the coevolution of two traits, gamete size m_i and mating trait investment r_i, in the two mating types x and y, in a large diploid population. These two traits are coded by many autosomal loci of small effect. The expression of each trait is linked to the mating type: each genotype carries the two trait values of the two mating types, defined by the vector $T = (m_x, r_x, m_y, r_y)$, but an individual will only express the trait values corresponding to its own mating type. Initially, we assume evolution to be under isogamic constraint, meaning that the two mating types x and y have equal gamete size $m_x = m_y = m_\mathrm{c}$ and equal mating trait investment $r_x = r_y = r_\mathrm{c}$. Under the isogamic constraint, the strategy of a genotype is thereby given by only two traits $T_\mathrm{c} = (m_\mathrm{c}, r_\mathrm{c})$, where c denotes the traits being under the constraint.

In our analysis, we consider a large resident population with a strategy T determined by many loci, which are initially all homozygous. We consider the iterative introduction of new mutations, each affecting arbitrarily one of the loci determining the strategy and producing a slight deviation in one or more of the traits. When the mutating locus is homozygous for the new allele, it leads to strategy T'_A. However, because new mutations are rare, they initially always occur as heterozygotes with the resident allele at that locus. Such mutant heterozygotes have the strategy $(T'_A + T)/2 = T' = (m'_x, r'_x, m'_y, r'_y)$. This assumption aligns with the locally additive genotype-to-phenotype mapping as described in Metz and de Kovel (2013).

To evaluate the initial invasion success of such a mutant allele, we only need to consider the reproductive success of the strategy of this mutant heterozygote T', as discussed in Metz and de Kovel (2013) and we refer to this strategy as the mutant

strategy. In the context of evolution under isogamic constraint, we replace T with T_c and T' with T'_c. The expected long term growth of such rare mutant strategy T' is given by its reproductive success F'_i (Eq. A14) divided by the reproductive success of the resident strategy F_i (Eq. A9), averaged for the two mating types x and y (Shaw and Mohler, 1953),

$$w(T', T) = \frac{1}{2}\left(\frac{F'_x(m'_x, r'_x, T)}{F_x(T)} + \frac{F'_y(m'_y, r'_y, T)}{F_y(T)}\right). \quad [4]$$

Note that the resident reproductive success F_i is not affected by the mutant strategy T', as the mutant is assumed to be rare. For the same reason, the mutant reproductive success F'_i is not affected by the mutant traits of the other mating type. We refer to $w(T', T)$ as the invasion fitness of the mutant strategy where the mutant is able to increase in frequency, and thereby invade, whenever $w(T', T) > 1$.

Adaptive dynamics. By assuming large population and rare mutations of small effect, we can use the adaptive dynamics framework to predict the evolutionary dynamics (Metz et al., 1992; Geritz et al., 1998; Metz and de Kovel, 2013). Large populations ensure close to deterministic dynamics, small mutational effect ensures that a mutant allele that invades will always replace and become the new resident allele as long as the population is under directional selection (Dercole and Rinaldi, 2008; Priklopil and Lehmann, 2020) and rare mutations ensure that a mutant allele will either fixate or go extinct before a new mutant is introduced. If a mutant allele T'_A fixates, its strategy will become the new resident strategy T of the population. This results in a trait substitution sequence where the strategy of the population T evolves in a step-wise manner for each invading mutant.

The selection gradient $\boldsymbol{\beta}$ is given by the gradient of the invasion fitness (Eq. 4) when the mutant strategy T' is similar to the resident strategy T,

$$\boldsymbol{\beta}(T) = \nabla w(T', T)\Big|_{T'=T}. \quad [5]$$

The selection gradient $\boldsymbol{\beta}$ gives the direction in the trait space of T in which mutants have the highest invasion fitness, and multiplied with the mutational variance-covariance matrix, it gives the expected direction of evolution. Within the limit of small mutational effect, iterating this mutation-invasion process results in a gradual evolutionary path given by

$$\frac{\mathrm{d}T}{\mathrm{d}t} = 2\mathsf{C}\boldsymbol{\beta}(T), \quad [6]$$

(Dieckmann and Law, 1996; Champagnat et al., 2006; Durinx et al., 2008; Metz and de Kovel, 2013), where C is the product of the mutation rate, effective population size and the mutational variance-covariance matrix on T' (examples of evolutionary paths obtained using Eq. 6 are found in the Result section in Figure 4). The factor two comes from the fact that as soon a mutant allele with strategy T' in heterozygote form has invaded and then fixated, it will be the resident in homozygote form with strategy T'_A providing twice the phenotypic changes of the heterozygote strategy T' (Metz and de Kovel, 2013).

For our analysis, we consider the traits to evolve proportionally at equal rates with C being equal to the identity matrix times one half (for details, see Appendix A5.1) and the evolutionary path (Eq. 6) is then given by the selection gradient (Eq. 5).

Predicting the evolutionary outcomes. We can predict the outcomes of the evolutionary path (as given by Eq. 6) using the adaptive dynamics framework. Strategies T where directional selection ceases, i.e $\boldsymbol{\beta}(T) = 0$, are of special importance. These

strategies are called singular strategies, and we denote them T^* (or T_c^* for evolution under the isogamic constraint). A singular strategy T^* has two important stability properties. First, convergence stability tells whether T^* is an attractor or a repeller of the evolutionary dynamics, i.e, whether trait evolution will approach it or not. Second, evolutionary stability tells whether T^* can be invaded by nearby mutant strategies. In Appendix A5.3 we give details on how we derive these stability properties for the four and two-dimensional trait spaces of T and T_c, respectively.

Each strategy of the isogamic constrained evolution $T_c = (m_c, r_c)$ has a corresponding isogamic strategy for the unconstrained evolution, namely $T = (m_c, r_c, m_c, r_c)$ and we denote this strategy $T_=$. Also, each singular strategy of the constrained evolution $T_c^* = (m_c^*, r_c^*)$ happens to also always be a singular strategy at its corresponding point in the unconstrained evolution $T_=^* = (m_c^*, r_c^*, m_c^*, r_c^*)$, due to the symmetry of the competition trait between the mating type (Supplementary information S2.1). This gives each isogamic singular strategy pair $(T_c^*, T_=^*)$ a total of four stability properties: the convergence stability and evolutionary stability of both the constrained and the corresponding unconstrained evolution.

The evolutionary process is as following: first, under the isogamic constraint, evolution reaches its attractor (singular point) T_c^*. Then, the constraint is released, and we see if the evolution diverges from $T_=^*$. Under this setting we can, as described below, classify the evolutionary dynamics at each singular strategy pair $(T_c^*, T_=^*)$ into different scenarios. For our model, four different scenarios for the singular strategy pair turn out to be important: it can either be a point that repels isogamic constrained evolution, or it can be an attractor of the constrained evolution in which case three outcomes are possible: evolution transitions from isogamy to anisogamy, evolution comes to a halt and the population stays isogamic, or genetic polymorphism evolves.

Classification of the evolutionary dynamics at isogamic singular point. To predict the evolutionary dynamics, we look at the properties of the isogamic singular strategies. We classify the evolutionary dynamics around each isogamic singular strategy pair $(T_c^*, T_=^*)$, where we first look at the convergence stability of T_c^* telling whether the constrained evolution will approach T_c^* in the first place or not. If T_c^* is a repeller it will not be approached by evolution and the other three stability properties (the evolutionary stability of T_c^* and the convergence and evolutionary stability of $T_=^*$) have no relevance. On the other hand, if T_c^* is an attractor, the isogamic constrained evolution will approach it and, two or potentially three different evolutionary outcomes can follow depending on the other three stability properties:

1) An attractor of the isogamic constrained evolution T_c^* is an evolutionary end-point if both T_c^* and its corresponding $T_=^*$ are attracting and uninvadable. Then when evolution reaches T_c^*, no further mutants can invade in either the constrained or unconstrained trait space. Hence, evolution stops and the population stays isogamic.

2) An isogamic attractor T_c^* is a point where anisogamy evolves if T_c^* is uninvadable, but $T_=^*$ is invadable and repelling for the unconstrained evolution. Then it is a special type of saddle point, being a fitness maximum in the isogamic constrained two-dimensional trait manifold but a fitness minimum in orthogonal directions (where the gamete traits of the mating types diverge) in the four-dimensional unconstrained trait manifold. This corresponds to disruptive selection for gamete size m_i and/or mating trait investment r_i to diverge between the two mating types x and y for the unconstrained evolution, which acts as a selection pressure for the removal of the isogamic constraint. As soon the isogamic constraint is removed, gamete size m_i and mating trait investment r_i of the two mating types x and y diverge and the population evolves anisogamy as it repels away from the isogamic strategy $T_=^*$. The mating type with larger gametes (arbitrarily) gets the index x, and is defined as female,

while the other mating type y is defined as male (i.e., $m_x > m_y$).

3) If an attractor of the isogamic constrained evolution T_{c}^* is both invadable by nearby mutants, and also an invadable repeller for the unconstrained singular strategy $T_{=}^*$, two different outcomes can follow. First, anisogamy can evolve removing the isogamic constraint, just as described above in case (2). Second, because T_{c}^* is an invadable attractor for the constrained evolution, it is a special point where isogamic genetic polymorphism can evolve: if T_c^* is reached by evolution and the isogamic constraint remains, nearby isogamic mutant strategies can invade and coexist with T_{c}^* resulting in two isogamic genotype strategies. The strategies of these two isogamic genotypes then diverge as evolution proceeds (evolutionary branching, Geritz et al., 1998, 2016). One genotype then evolves larger gametes (with equal size for both mating types) and the other evolves smaller gametes (still equal size for both mating types). Hence, this introduces genetic variation in gamete size in the population becoming pseudo-isogamic, as this gamete size polymorphism within mating types can be seen as an anisogamous situation, but with each genotype remaining isogamous. However, if the isogamic constraint is removed because anisogamy is favoured by selection, the possibility for isogamic genetic polymorphism is ruled out, and there is indeed evidence that the evolution of isogamic polymorphism is unlikely if anisogamy is allowed to evolve, as anisogamy will evolve first, prohibiting the evolution of isogamic polymorphism (Van Dooren et al., 2004). For the scope of this manuscript we will report whenever the suboptimal pseudo-isogamic genetic polymorphism can evolve, but we will focus on the evolution of anisogamy assuming it to be the final evolutionary outcome.

By classifying the evolutionary dynamics for all isogamic singular strategy pairs in this way, we can predict the evolutionary outcome. For a given parameter combination, we first numerically solve for the singular strategies (Appendix A5.2) and then derive their convergence and evolutionary stability (Appendix A5.3). We report if these attractors are points where evolution either (1) stops resulting in stable isogamy, (2) transitions into anisogamy, (3) transitions into either anisogamy or pseudo-isogamic genetic polymorphism. We iterate this procedure for a wide range of scenarios by systematically varying the parameters of the model.

A special case occurs if there is a single attractor of the isogamic constrained evolution $T_{\mathrm{c,a}}^*$ with negative and real eigenvalues, and there are either no other singular points, or alternatively if all other singular points, which are repellers ($T_{\mathrm{c,r1}}^*, T_{\mathrm{c,r2}}^*, \ldots$), are located on the edge of the trait space (occurs for minimum gamete size $m_{\mathrm{c,r}i}^* = 1$, no mating trait investment $r_{\mathrm{c,r}i}^* = 0$, or full mating trait investment $r_{\mathrm{c,r}i}^* = 1$). Then, we find $T_{\mathrm{c,a}}^*$ to be an unequivocal destination of the isogamic evolution. In all other cases, there might be multiple evolutionary outcomes, and which one is reached might depend on the initial trait value from where evolution starts and the mutational covariance matrix C. Conveniently, we find that for any set of parameters within our investigated parameter ranges, this special case holds, such that there is always a single isogamic attractor $T_{\mathrm{c,a}}^*$ to which evolution converges, independently of from where it starts.

If anisogamy evolves (cases (2) and (3)) after reaching the isogamic attractor $T_{\mathrm{c,a}}^*$, the isogamic constraint is removed, leading to an increase in the number of evolving traits from two: $T_{\mathrm{c}} = (m_{\mathrm{c}}, r_{\mathrm{c}})$, to four: $T = (m_x, r_x, m_y, r_y)$. While we can numerically determine all isogamic singular strategies, solving for the singular strategies of the unconstrained evolution ($T_1^*, T_2^*, \ldots$) becomes hard due to the high dimensionality of this trait space. Therefore, to get the evolutionary endpoint after anisogamy evolves, we have to rely on numerically solving the evolutionary path (Eq. 6).

Numerically solving for the evolutionary path. In parallel with analysing the isogamic singular strategies predicting the evolutionary outcomes, we also numerically solve for the evolutionary path given by Eq. 6 (as described in Supplementary information S2.3). For completeness, we start by solving for the evolutionary path under the isogamic constraint, and verify that evolution leads to the isogamic attractor $T^*_{\mathrm{c,a}} = (m^*_{\mathrm{c,a}}, r^*_{\mathrm{c,a}})$. Then, we continue the numerical solution without the isogamic constraint, starting at the corresponding singular point of the unconstrained evolution $T^*_{=} = (m^*_{\mathrm{c,a}}, r^*_{\mathrm{c,a}}, m^*_{\mathrm{c,a}}, r^*_{\mathrm{c,a}})$, and thereby allow anisogamy to evolve (ignoring the possibility for isogamic polymorphism to evolve in case (3) as mentioned above). If $T^*_{=}$ is an attractor no evolution follows, the population stays isogamic, and we conclude that $T^*_{\mathrm{c,a}}$ was an isogamic end-point of evolution. On the other hand, if $T^*_{=}$ is a repeller, trait values for the different mating types diverge away and anisogamy evolves.

Finally, we continue the unconstrained evolutionary path until it stabilizes at an anisogamic attractor $T^*_{\mathrm{a}} = (m^*_{x,\mathrm{a}}, r^*_{x,\mathrm{a}}, m^*_{y,\mathrm{a}}, r^*_{y,\mathrm{a}})$ giving us the anisogamic end-point of evolution (a fixed point attractor), or until evolution stabilize in an oscillating cycle (a limit cycle attractor). Since we could not solve for the anisogamic singular strategies, numerically solving for evolutionary path gives us additional results that we could not obtain with the stability analysis of singular point presented above.

Parameter reduction and gamete density. We find that the number of parameters can be reduced down by four when analysing the evolutionary dynamics of the model. Five of the parameters (d, e, p, t_{end} and v_0) always occur as a product together in the invasion fitness function (Eq. 4) and thereby also in the selection gradient (Eq. 5) as well as in the evolutionary path (Eq. 6). Hence, when analysing the evolutionary dynamics, we can substitute their product into a single parameter $\delta = d \times e \times p \times t_{\mathrm{end}} \times v_0$.

Varying the parameter δ is the same as varying one or more of the five parameters of its product, all increasing how likely gametes are to get fertilized. It can correspond to varying the gamete density, as it contains $d \times e$: the two parameters being proportional to the initial gamete density $n_{i,0}$. Furthermore, δ contains $t_{\mathrm{end}} \times v_0$ which is proportional to the distance travelled per gamete, and also p the probability of a collision resulting in fertilization. All five parameters encapsulated in δ have identical effects on the evolutionary dynamics (as they occur together in a product): they regulate whether the system tends towards low encounter rates resulting in high levels of gamete limitation at low values of δ, or high encounter rates resulting in low levels of gamete limitation at high values of δ. From now on, for the sake of simplicity, we will refer to δ as the gamete density constant ($d \times e$), assuming the other parameters (p, t_{end}, and v_0) to be fixed. Note that when we vary the gamete density constant $\delta = d \times e$, it can both correspond to changing from low to high population density d, or from low to high amount of energy allocated to gamete production per individual e.

Results

Here, we present how two gametic traits, gamete size m_i and investment r_i into a mating trait, coevolve in a population with two mating types x and y. We begin with some general results of the stability analysis, giving insights about the transition from isogamy to anisogamy. Then, we present the results gained from solving for the evolutionary path (Eq. 6) of the gamete traits $T = (m_x, r_x, m_y, r_y)$. When performing the analysis, we vary the model parameters, δ, K_g, K_z, and α_m (or α_d for the fusion partner capture scenario) to represent a wide range of scenarios. A subset of the analysed parameter range is presented in Figure 5, showing the result for a high K_z (zygote survival highly size-dependent) which appears as the most biologically relevant scenario. In Supplementary Figures S1-S2 we also show results for K_z intermediate and absent.

Transition from isogamy to anisogamy. For our investigated parameter ranges (Figures 5 and Supplementary Figures S1-S2), there is a single isogamic attractor $T^*_{\mathrm{c,a}}$ to which the isogamic constrained evolution converges. We find that the evolution either stops at this attractor $T^*_{\mathrm{c,a}}$ and the population stays isogamic (Figure 4**a**) or selection turns disruptive for the gamete traits of the two mating types x and y. This disruptive selection results in divergence of the gamete sizes, m_x and m_y, and usually also of the mating trait investments, r_x and r_y, and anisogamy evolves (Figure 4**b-d**). For both types of mating traits (motility and fusion partner capture), we show in Figures 5 and S1-S2 the parameter regions where evolution leads to isogamy (within dashed contour lines) or anisogamy (outside dashed contour lines). This shows that anisogamy is very common at lower gamete density (below $\delta = 1$), which is not a surprise because anisogamy favours gamete encounters in that context (Dusenbery, 2006). At higher densities, there is always a possibility for isogamy to remain, depending on complex interactions between the mating trait, the relationship between trait efficiency and gamete size and the size-survival parameters K_g and K_z.

For a considerable subset of the parameter region where the evolution of anisogamy is expected, there is the possibility for the suboptimal pseudo-isogamic genetic polymorphism to evolve (outlined with gray contours in Figures S1-S2). In that case, the isogamic attractor is invadable under the constrained evolution, which can result in two diverging isogamic genotypes, one producing large gametes (of both mating types) and the other producing small gametes. However, in line with Van Dooren et al. (2004), we assume that anisogamy evolves first, ruling out the possibility for polymorphism to evolve (see more details in the Analysis section).

The evolutionary path of the gamete traits in two mating types. Solving for the isogamic singular strategies and analysing their evolutionary stability told us whether anisogamy evolves or not. In addition, we solve numerically for the evolutionary path (Eq. 6) finding the trait values at the anisogamic endpoint of evolution $T = (m_x, r_x, m_y, r_y)$. The outcomes of the evolutionary path analysis matches our predictions of the stability analysis. For the parameter regions where the evolutionary path leads

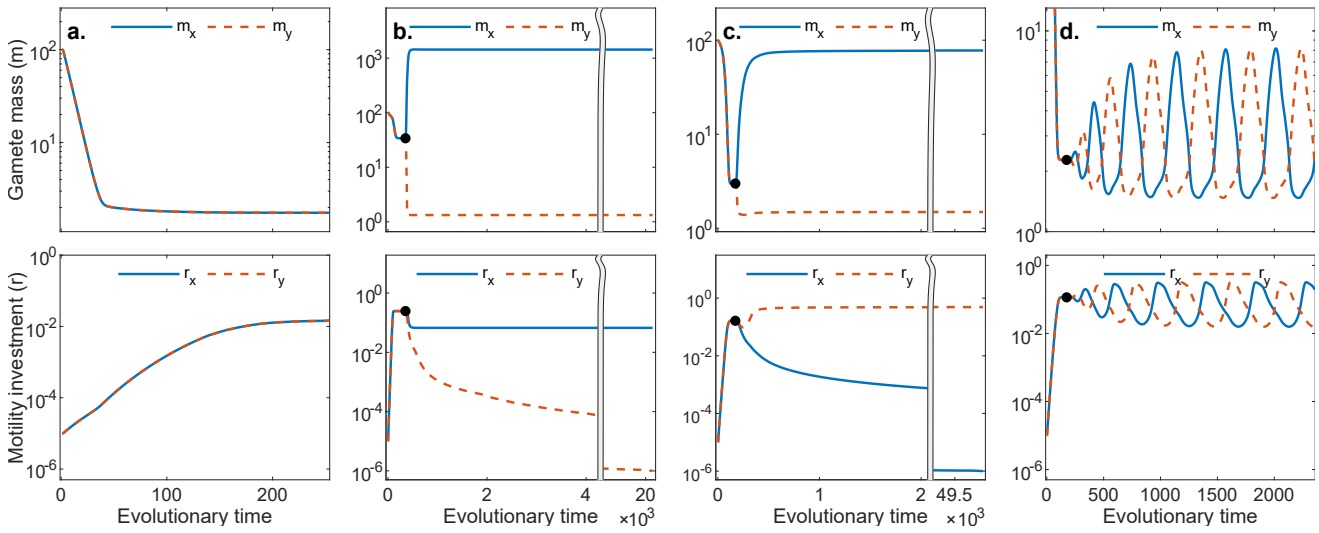

Fig. 4. Four examples of the evolutionary path of the gamete traits depicting qualitatively all possible evolutionary outcomes of the model: **a.** no evolution of sexual dimorphism in gamete size or mating trait, **b.** evolution of anisogamy with female-biased mating trait investment, **c.** evolution of anisogamy with male-biased mating trait investment and **d.** oscillating evolutionary dynamics (limit cycle) alternating between female-biased and male-biased mating trait investment. In each graph, the horizontal axis represents evolutionary time in equation 6, and the vertical axis gives trait value for gamete mass (top panels) and mating trait investment (bottom panels). Values are given for the two mating types x (blue, full line) and y (orange, dashed line). If stable anisogamy evolves (cases **b.** and **c.**), the mating type with the larger gamete size is called female, denoted x (blue), and the one with smaller gametes is called male, denoted y (orange). Parameters: $K_g = 0.1$, $K_z = 10^4$, $a_m = 1$, and $\delta = (10^2, 10^{-2}, 0.5, 1.5)$ respectively for **a.**-**d.** (these parameter combinations are found in Figure 5).

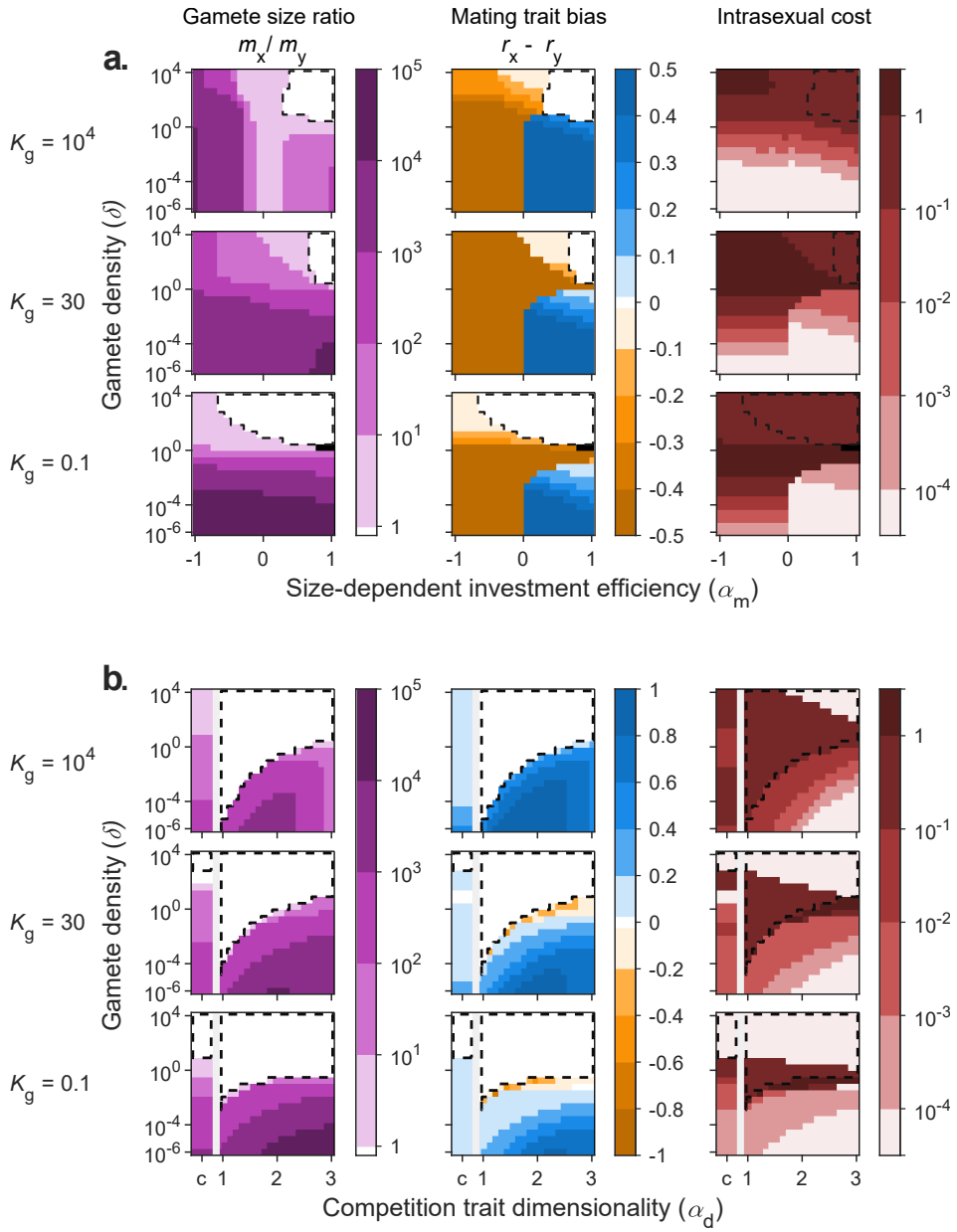

Fig. 5. Sexual dimorphism in gamete size, sex-bias in mating trait investment between the two mating types x and y and intrasexual cost of the mating trait for the case of motility (**a.**) and fusion partner capture (**b.**). The vertical axis of each subplot represents the gamete density constant δ. In (**a.**), the horizontal axis of each subplot represents the size-dependent investment efficiency α_m, which modulates whether gamete size has a positive or negative effect on the efficiency of energy invested into motility. In (**b.**), the horizontal axis of each subplot represents the dimensionality parameter α_d ranging from 1 to 3, which determines how costly the physical structures are (low α_d means low cost). The left part of each plot in (**b.**) is reserved for the special case of chemoattraction, denoted by a c on the plot axis and separated by a gray bar from the physical structure case. The dashed line comes from derivations of the stability analysis and encapsulates the area where isogamy is the expected evolutionary end-point; in the remaining area, anisogamy is expected. The results from solving the evolutionary path are represented by the coloured shading showing the degree of sexual dimorphism in gamete size in purple (first column) or investment in the mating trait in orange for males-biased and blue for females-biased (second column) reached at the evolutionary endpoint, where white represents no dimorphism, and deep colours represent strong dimorphism. The last column gives the intrasexual cost of the mating trait in red, which quantifies the intensity of mating competition as a reduction in fitness imposed by the mating trait on individuals of the same mating type (details are given in Supplementary information S2.6). For anisogamic parameter region, the intrasexual cost is evaluated for the mating type investing more into the mating trait. We present results for a high value of K_z ($K_z = 10^4$), meaning that zygote survival is highly dependent on zygote size, and for three values of K_g, the size-dependent survival parameter for gametes.

to anisogamy, we present the degree of gamete size-dimorphism measured as the ratio of gamete sizes of the two mating types m_x/m_y, and the sex-bias in mating trait investment measured as the difference $r_x - r_y$ in Figure 5 and Supplementary Figures S1-S2. We note that for all the parameter regions explored with motility and the large majority with fusion partner capture, only one mating type invests in the mating trait for a given evolutionary scenario, so that the absolute value of the investment bias also gives the mating investment r_i for the mating type that invests. We find that four qualitatively different types of anisogamic outcomes are possible. The first two outcomes are anisogamy with either female-bias ($r_x > r_y$, Figure 4b) or male-bias ($r_x < r_y$, Figure 4c) in mating trait investment represented as blue or orange regions, respectively, in Figure 5 and S1-S2b. Third, for the case of chemoattraction in the fusion partner capture model, there is a restricted parameter region within the anisogamy space where only one of the two gamete traits (either size or mating trait investment) diverges between the mating types. This is visible as a white pixel outside the dashed contour line on Figure 5b left panel ($m_x = m_y$, size does not diverge) and right panel ($r_x = r_y$, mating trait investment does not diverge). Finally, there are some very restricted parameter regions where the anisogamic attractor is a limit cycle, resulting in never ending oscillating dynamics (Figure 4d). In some of these cases, we have smaller non-symmetric oscillations where the mating types stays separated such that one consistently has larger gamete size than the other. We then report averaged trait values over several oscillation periods. Otherwise, the oscillations are large and symmetric, such that the mating types alternate which is the larger (female) and the smaller (male), as in Fig. 4**d**; these are represented as black regions in Figures 5 and S1-S2 (just a few pixels in total). In the next subsections, we detail the influence of the model parameters on the evolution of anisogamy and sex-bias in investment for each mating trait. We vary the gamete density constant δ which alters the level of gamete limitation, and the gamete and zygote size-survival parameters, K_g and K_z. We focus on parameter regions where mating competition occurs to investigate the relationship between anisogamy evolution and sex-biases in competition for mating. We consider that significant competition occurs from an intrasexual cost of 10^{-2} and higher in Figures 5 and S1-S2. A cost of 10^{-2} means that if other individuals of the same mating type increase their investment in the mating trait (without trade-off), a focal individual gets a relative reduction in fitness corresponding to a one-hundredth of this increase.

General trends of sex-bias in mating competition. Focusing on the parameter spaces where anisogamy evolves, we start by highlighting some general trends across the two types of mating traits (Figure 5a and b, and Figures S1-S2). At high gamete density ($\delta >> 1$), anisogamy only evolves if the mating trait is efficient in small gametes, and anisogamy evolution requires in addition that at least one of the size-survival parameters is high (see Figures S1-S2). At high density, anisogamy is thus limited to the motility scenario with low α_m (Figure 5a), and is accompanied by a high intrasexual cost of the mating traits, indicating mating competition. We propose that anisogamy emerges in this context because there is a trade-off between maximizing gamete or zygote survival and maximizing mating competition efficiency. The trade-off only occurs if the mating trait is more efficient in small gametes, which is only found for the motility trait with $\alpha_m < 0$. This leads to specialization of small gametes into the mating competition trait, and of large gametes into fertilisation targets as well as into zygote provisioning when K_z is high. When the mating trait is more efficient in large gametes ($\alpha_m > 0$), there is no trade-off and the population stays isogamic where all gametes evolve to be large.

As density δ decreases, there is an area of parameter space, starting from around $\delta = 1$, where anisogamy also evolves when the mating trait is more efficient in large gametes, *i.e.* in the motility scenario with $\alpha_m > 0$ and in the fusion partner

capture scenario (Figure 5b). In this region, there are many instances where the intrasexual cost of the mating trait is still high, indicating mating competition. Competition occurs when there is either a strong gamete survival constraint (top row in Figure 5a and b) or a weaker zygote survival constraint (subplots in Figure S1 and S2 where either $K_z \leq 30$ or $K_g = 10^4$). Importantly, at these intermediate densities, female biased mating competition occurs, meaning that females can invest more energy than males into a mating competition trait. We suggest that in these cases disruptive selection on size may be driven by decreasing encounter rates as density δ lowers. At very low densities ($\delta << 1$), the intrasexual cost of the mating trait becomes negligible so that the mating trait is primarily a trait maximizing gamete encounter rates under extreme gamete limitation rather than a competition trait. However, when the mating trait is highly energy efficient (e.g., chemoattraction, or low α_d for fusion partner capture by physical structures), competition can still occur at very low density, likely because the high efficiency of the trait attenuates the effect of gamete limitation. In these particular cases as well, females invest more than males into a mating competition trait (chemoattraction case in both Figure 5**b** top row, and in Figure S2 where either $K_z \leq 30$ or $K_g = 10^4$).

When K_g is low and K_z high, we observe the strongest anisogamy because there is no cost in having small gametes but a high cost in having a small zygote (Figure 5**b** two bottom rows, and in Figure S2 where both $K_z = 10^4$ and $K_g \leq 30$). Because of the fixed energy budget for gamete production, this strong size difference leads to a large difference in gamete numbers between mating types, which magnifies gamete limitation. In that special case, the intensity of competition is much reduced when the mating trait investment r_i transitions from male-biased to female-biased. This means that strong constraint of zygote size on survival and low constraint of gamete size on survival create conditions where competition for mating can evolve primarily in males.

When motility is more efficient in small gametes. The scenario of a motility mating competition trait with $\alpha_m = -1$ corresponds to the force of propulsion being invariant to gamete size, leading to increased speed for smaller gametes due to reduced drag. This type of size-speed relationship is observed among gametes within genera (Dusenbery, 2009, chapter 20, Table 20.1). In this case, with high K_z we observe that anisogamy evolves from low to high gamete density, and is always accompanied by male biased investment in the mating trait (Figure 5a). Only in the case where both K_g and K_z are low does anisogamy not evolve at high densities (Figure S1), simply because there is no limitation imposed on gamete size by survival and both mating types can produce small and efficient motile gametes leading to viable zygotes.

When motility is more efficient in large gametes. The other scenario for motility corresponds to $\alpha_m = 1$, which is the mechanistically explicit case when thrust increases proportionally to gamete volume, a size-speed relationship that is consistent with trends observed across small water organism of vastly different genera and sizes (Dusenbery, 2009, Fig. 8.3) as well as in gametes across genera (Dusenbery, 2009, Table 20.1). In this case, anisogamy does not evolve at high densities. When anisogamy evolves, at lower densities, it most often leads to female biased investment in the mating trait, except for a restricted range of intermediate densities that shows male-biased investment, when $K_g < K_z$ (Figure 5a and Figure S1). The condition $K_g < K_z$ is generally expected to encourage anisogamy and male competition because zygote survival strongly depends on size, while there is no strong dependency of gamete survival on size.

Fusion partner capture by physical structures. In this scenario, gametes can produce an increase in apparent size with a cost proportional to the increase in the volume of its jelly coat ($\alpha_d = 3$), the surface of the cell membrane surface ($\alpha_d = 2$) or the cell radius ($\alpha_d = 1$). Comparable to the motility case with $\alpha_m = 1$, physical structures are more efficient in large gametes (with $\alpha_d = 1$ having the highest efficiency), and the outcome is qualitatively similar: anisogamy only evolves at relatively lower densities, paralleled by female biased investment in the mating trait (Figure 5b and Figure S2), except for a restricted space of male biased investment that appears at intermediate densities when $K_g < K_z$. Whenever the intrasexual cost of the mating trait is high ($> 10^{-2}$), it reveals competition for mating. Mating competition and anisogamy co-occur at intermediate density and when investment into the mating trait is sufficiently energy efficient in large gametes (α_d is low enough). As for the motility trait, female biased investment in a mating competition trait evolves when either K_g is high, or K_z is low (Figure 5**b** top row and Figure S2 where either $K_z \leq 30$ or $K_g = 10^4$).

Fusion partner capture by chemoattraction. With chemoattraction, gametes can extend the range in which they can be detected, and is only effective in the mating type with the larger detection zone. For this reason, chemoattraction can only benefit one mating type, which creates an inherent asymmetry. This mating trait is more efficient in large gametes, in the same degree as the physical structures with $\alpha_d = 1$, but allows for the evolution of anisogamy at higher density than for physical structures. It can also, rarely, lead to cases where only one of the gametic traits diverges (either gamete size or mating trait investment), which is not seen in any of the other mating traits. Even at low densities, the intrasexual cost of chemoattraction is high, which supports the view that mating competition traits can easily evolve in females in nature, where chemoattraction is a widespread feature of female gametes.

Conclusion We highlight some overarching results: (i) when anisogamy evolves it seems to almost always be accompanied by a sex-biased investment in the mating trait, (ii) whereas only male-biased investment in the mating trait can evolve under high gamete density, both male and female bias investment can evolve at intermediate densities, and finally, (iii) female-biased investment in the mating trait also appear in areas where the trait has a strong competition component (chemoattraction being the most striking case). At lower densities, either sex may evolve mating traits, but the intensity of mating competition becomes negligible because of extreme gamete limitation. We have seen that the relationship between gamete size and trait efficiency is key in determining the resulting sex-bias in investment into the mating trait, which may appear as self-evident. However, we advocate that this result is still meaningful, in showcasing the variety of mating competition traits that may arise by chance, some more efficient in large gametes and some in small gametes. The special case of chemoattraction is insightful, in revealing that some types of traits are prone to producing asymmetries in selection pressures between the mating types. Examining this diversity is necessary to fully understand the relationship between the evolution of anisogamy and that of mating competition traits. On the contrary, making the restrictive assumption that competition should only arise in small gametes (by only considering motility with negative α_m values for example) can lead to the conclusion that males should invest more into competition, but this view leaves many possible scenarios aside. With these other mechanistic traits, we show that the evolution of anisogamy and sex-bias in mating competition investment is also possible when competition happens through a trait favouring female strategies (large gametes). We elaborate more on this point in the discussion.

Discussion

Two pathways to anisogamy and resulting sex-bias in competition for fertilization. We have presented a mechanistic model of mating competition for fertilization, in which gamete size and a mating trait that increases adult reproductive success coevolve. The mechanistic nature of our model allows us to describe mating traits with a clear biological function. Our work shows that anisogamy often evolves along with a sex-biased investment in mating traits. This is true for the different types of mating traits investigated here, first, gamete motility that may be more efficient in either small or large gametes, and second, fusion partner capture modelled as either physical structures or chemoattraction. Previous work has shown that anisogamy may have evolved under *gamete competition* (high gamete density and absence of gamete limitation) or *gamete limitation* (not all female gametes are fertilized) (e.g. Bulmer and Parker, 2002; Lehtonen and Kokko, 2011; Hoekstra et al., 1984). We believe that this distinction is important because the forces of selection that would have acted to produce gamete size differences in these two scenarios are not the same. This has implications for the evolution of traits involved in mating competition, which we investigate here. This question is relevant to the initial evolution of anisogamy from an isogamous state, but also to the maintenance and continuous evolution of gamete size in contemporary species, as we discuss later.

In the absence of gamete limitation, under high gamete densities, the forces that are expected to drive the evolution of anisogamy are size-dependent survival selection of both gametes and zygotes, and competition for fertilization success. In that context, anisogamy should only evolve under a size constraint on survival. If anisogamy does evolve, all large gametes become fertilized, but smaller ones are in excess, leading to the evolution of male-biased investment in intrasexual competition. In essence, the dimorphism in gamete size and number that evolve in the absence of gamete limitation can already be thought of as parental investment and competition traits for females and males respectively. Under extreme gamete limitation, corresponding to very low gamete densities, the force expected to drive the evolution of anisogamy is disruptive selection on gamete size, maximizing encounter rates of gametes from the two mating types. In that context, both sexes could be expected to invest in a trait increasing encounter rates because they may both have unfertilized gametes at the end of a mating event (Evans and Lymbery, 2020).

By adjusting gamete density, our model allowed the exploration of intermediate ranges of gamete limitation. We have seen again that anisogamy may evolve in different contexts, implying different intensities of competition for mating and with different outcomes in terms of the sex-bias in investment into the mating traits. Very high gamete density clearly favoured the evolution of a male-bias in mating competition. But the evolution of anisogamy in that context was restricted to a parameter region where the mating trait is more efficient in smaller gametes. Anisogamy evolution was also encouraged at high density by a strong size-dependence of gamete and zygote survival (as in Bulmer and Parker, 2002 for the latter). On the other hand, intermediate gamete densities allowed both sexes to invest in mating competition, with the final sex-bias largely determined by the nature of the mating trait, more specifically whether it was defined as more cost-efficient in smaller or larger gametes. This result highlights that the evolution of anisogamy needs not result in the evolution of a competition traits in males, but may lead to a variety of outcomes depending on the circumstances under which anisogamy initially evolved and which trait is considered. Importantly, we also showed that the evolution of female-biased investment in a mating competition trait was not limited to parameter spaces where gamete density is so low that mating competition is negligible. Although competition intensity does decrease with decreasing gamete density, transitioning from male-biased to female-biased investment in the

trait only reduced the intensity of competition in the parameter space where the gamete and zygote size-survival parameters encouraged larger anisogamy ratios. This trend may be due to the gamete size-number trade-off imposed by the fixed energy budget. These results indicate that some moderate level of gamete limitation could allow females to invest more energy than males into competition traits in contexts where mating competition is a driver of the trait evolution.

In contrast, in the only other model studying this same question, Lehtonen et al. (2016) find that competition trait evolution should always be favoured in males under most scenarios, although the authors acknowledge that it could be equally favoured in males and females under severe gamete limitation. This discrepancy between their results and ours stems from a difference in the component of fitness from which the sex-specific asymmetries that lead to the evolution of sexual dimorphism in competition arise. We advocate that sex-specific asymmetries in selection are generally more likely to arise from individual competition components than from group-level fecundity. In terms of evolutionary dynamics, the effect of a mutant strategy on group-level fecundity becomes negligible as group size increases, while the effect of competition remains important in determining individual relative fitness for any group size (Supplementary information S2.5.2). We provide more details of how fitness is expressed in the model of Lehtonen et al. (2016) and in ours in Supplementary information S2.5.

Competition traits in the model and in nature. We implemented in our model two possible mating traits. Although those traits are gamete-level traits, we remind the reader that they are equivalent to classical sexually selected traits that increase the reproductive success of the bearer, only adapted to the biology of broadcast spawners. Both traits are flexible with the addition of one parameter that allows to describe different mechanistic scenarios. The motility trait can either be more efficient in smaller or larger gametes, two relationships that have received empirical support on different levels (e.g. Dusenbery, 2009, Fig. 8.3 and Table 20.1). The fusion partner capture trait can be described with different cost dimensionalities, corresponding to cost of producing jelly coat, membrane or a cellular function that scales with an increase in radius. We also consider the case of chemoattraction, which has a low cost and scales with the radius but only provides function in the mating type with the largest chemoattraction radius.

We have seen that the nature of the efficiency relationships of the traits greatly influences the resulting sex-bias in selection in our model. In particular, the trait gamete motility evolves in males at high gamete densities and can evolve in either sex at intermediate densities, depending on the relationship between trait efficiency and gamete size. In short, if small gametes benefit more from investing in that trait, then motility will be male-biased and *vice versa*. The fact that few free swimming eggs have been observed in nature so far (Motomura and Sakai, 1988; Klochkova et al., 2019) suggests that small gametes may generally swim more efficiently than large ones. However, motility is not a universal feature of sperm (Morrow, 2004), and eggs as well as sperm may benefit from assisted motion from the female or male individual that produce them (Gorelick et al., 2017). We also note that a positive relationship between size and speed of gamete emerges from the most parsimonious mechanistic description of motility in water, and is supported by across genera comparisons of swimming organisms (Dusenbery, 2009, Fig. 8.3) and gametes alike (Dusenbery, 2009, Table 20.1). A positive relationship between gamete size and speed has also been reported within genera in a unicellular algae (Seed and Tomkins, 2018), but this relationship may not hold for size differences of a thousand-fold or more, as is often the case in anisogamous systems.

Regardless, our goal with this model was not to accurately describe the physics of gamete motility as found in nature, but rather to provide a biologically relevant trait that could either be more cost-efficient in male or female gametes by variation of

one parameter. Consequently, we admit that swimming egg are rarely observed and therefore may be unrealistic, but this should not undermine the conclusion that sex-specific cost-efficiency of the trait drives the evolution of mating competition in the intermediate density scenarios.

To further this point, it is easy to imagine other biologically relevant traits that could be realistically less costly to develop for larger gametes. With that in mind, we incorporated in our model a second type of trait, fusion partner capture. This type of trait increases the apparent volume of the gamete, making it a larger fertilization target without increasing its survival probability. In our model, such traits develop mainly in the mating type producing the larger gamete, resulting in female-biased competition investment. This trait type can be compared to the egg jelly coat found in several species of broadcast spawning marine invertebrates (e.g. Podolsky, 2002; Farley and Levitan, 2001), and seems therefore quite realistic. Chemoattraction, which provides the most striking example of female mating competition in our model, is a common way for gametes to increase their apparent size in nature (Jantzen et al., 2001). This strategy is found in the eggs of several species, both external and internal fertilizers, including mammals (Eisenbach and Giojalas, 2006).

Prevailing forces in the evolution and maintenance of anisogamy in animals. In our model, the evolution of anisogamy is almost always accompanied by a sex-biased investment into the mating trait, but high or low gamete densities allowed for different outcomes. It is thus important to discuss what can be the respective importance of these different contexts in the evolution and maintenance of anisogamy. The current theory on the evolution of anisogamy proposes that it likely originated in sessile broadcast spawners (Parker, 2014), types of animal that are often subjected to gamete limitation (Levitan, 1996). This then suggests that gamete limitation may have been important in the evolution of an initial sexual dimorphism in gamete size. According to our results, this scenario can lead to either female or male-biased competition investment, depending on the nature of the mating trait considered. It seems therefore unlikely that the evolution of anisogamy should have generally resulted in male-biased investment into mating competition traits in early anisogamous animals.

Whether the sex-bias in mating competition investment at the initial anisogamy has an influence on the patterns of sex-specific competition in contemporary anisogamous species is unclear. The complex patterns of sex-specific selection that we observe today may be subjected to an array of confounding factors that we do not account for, such as evolutionary history or ecological constraints. Nevertheless, we need to comment, with our findings in perspective, the fact that in the majority of natural systems studied today more intense intrasexual competition is found in males than in females (Janicke et al., 2016; Janicke and Morrow, 2018). First, the claim of a general male-bias in mating competition should be nuanced: although males experience more intense intrasexual competition in a majority of species (Janicke et al., 2016; Janicke and Morrow, 2018), there is a lot of variation among taxa, as clearly visible from Figure 1 in Janicke et al. (2016). Females do experience non-negligible levels of intrasexual competition in most species, and in some cases more than males (reviewed in Hare and Simmons, 2018). Female competition is favoured if males provide costly nuptial gifts or parental care, but they may also compete to increase fertilization success in sperm limited-contexts (Hare and Simmons, 2018), which are not restricted to external fertilizers (see for example one study in gorillas Niemeyer and Anderson, 1983, and one in saiga antelopes Milner-Gulland et al., 2003). Second, we propose two non-mutually exclusive hypotheses that may explain the apparent inconsistency between our theoretical claim about the origin of anisogamy and empirical observations of today's natural systems. (i): a large proportion of animals studied by biologists are internal fertilizers. The evolution of internal fertilization reduces the chances for gamete limitation to appear,

which in turn should favour the evolution of male competition. (ii): our model assumes that individuals invest the same amount of energy into reproduction regardless of their sex or mating type. This assumption is common to all models of the evolution of anisogamy and stems from the fact that we start from an isogamous population, where the two mating types have the same reproductive strategy. If that assumption does not hold after anisogamy evolves however, and if the cost of producing larger gametes does not scale linearly with gamete size, it is possible that a difference in potential reproductive rate (PRR, time required for an individual to produce offspring and return to the mating pool, as in Clutton-Brock, Clutton-Brock and Parker, 1992) arises between the sexes. A sex-bias in PRR, leading to a sex-bias in time out of the mating pool (or "dry time", *sensu* Kokko et al. 2012) is likely to cause a sex-bias in intrasexual competition, with the sex with the highest PRR competing for mating opportunities with the other sex (Clutton-Brock and Parker, 1992; Kokko et al., 2006, 2012). We note that these two hypotheses (i) and (ii) do not undermine the fact that anisogamy (gamete size dimorphism) is not likely to explain directly sex-biases in intrasexual competition: in the first case it is the evolution of internal fertilization that causes males to compete more than females, in the second case it is a sex-bias in PRR, which could arise from anisogamy as well as from other causes. For example, PRR is highly sensitive to ecological factors, and field studies have shown that sex-biases in PRR can switch within the course of a single mating season (Almada et al., 1995; Forsgren et al., 2004, reviewed in Ahnesjö et al., 2008; Kvarnemo and Ahnesjo, 1996).

If it seems likely that gamete limitation played an important role in the evolution of anisogamy in ancestral animals, we can also wonder what are the evolutionary forces that maintain anisogamy in contemporary species. We have suggested above that the evolution of internal fertilization should have created a context with no or low gamete limitation (i.e., *gamete competition*) favourable to male competition. This claim should, however, be taken with care (Parker, 1982). A recent study in mammals has shown an inverse relationship between body size and sperm cell size (Lüpold and Fitzpatrick, 2015), a trend suggesting that in larger mammals, gamete limitation may happen to some extent, leading to the evolution of smaller more numerous sperm cells, less competitive but increasing chances of fertilization under low gamete density. Sperm limitation, or failure of females to get all of their eggs fertilized, may also be more common than expected in insects (reviewed in García-González, 2004). Finally, many contemporary invertebrate marine species are broadcast spawners that are often subjected to gamete limitation (Levitan and Petersen, 1995). In these species, variance in reproductive success may become higher in either sex depending on gamete density (Levitan, 2004), indicating that intrasexual competition may easily arise in either sex, as suggested by our results. Even though empirical explorations of sexual selection in broadcast spawners are rare (Evans and Sherman, 2013; Evans and Lymbery, 2020), several laboratory and field experiments have reported female traits that increase fertilization success and could therefore be involved in female intrasexual competition. In three species of sea urchins (Levitan, 1993, 1998*a*) egg traits are shown to evolve to maximize fertilization success. In the sea urchin *Lytechinus variegatus* experimental removal of a jelly coat around the eggs lowers fertilization success due to reduced target size (Farley and Levitan, 2001). In the sand dollar *Dandraster excentricus* a jelly coat that increases up to sixfold the size of the egg increases fertilization success (Podolsky, 2002), and finally in the tunicate *Styela plicata* (Crean and Marshall, 2008) both sexes adapt their gametes to population density, with female gametes becoming notably larger at low density, a strategy that increases fertilization success but comes at a cost for zygote survival. It is important to note that these female traits presumably evolved to increase fertilization success and not offspring survival, which clearly designates them as mating competition traits. Additionally, Marshall and Evans

(2005) showed experimentally that selection should act on females to increase fertilization success in the broadcast-spawning polychaete *Galeolaria caespitosa*.

Conclusion. We advocate that the importance of gamete limitation in shaping anisogamy should not be overlooked, which means that the evolutionary forces that are responsible for gamete size differences cannot be expected to always result in the evolution of male-biased mating competition investment. We thus question the claim that anisogamy necessarily favours the evolution of male-biased competition traits. Some of the evolutionary forces that spur the evolution of anisogamy in the *gamete competition* context do clearly favour male-biased competition traits; but evolutionary forces that shape anisogamy under different degrees of gamete limitation may produce male-biased or female-biased competition, with the outcome mostly decided by the nature of the competition trait and how its efficiency relates to gamete size. There are good reason to think that gamete limitation played an important role in the animals that first evolved the male and female sex. Even though the evolution of internal fertilization may have attenuated gamete limitation in a wide range of species, there is evidence claiming that even in internal fertilizers the evolutionary forces of gamete limitation are still at play. Together, this suggests that, as far as anisogamy is concerned, females should benefit from competing for increased fertilization success, too, a claim that is supported by the observation of female intrasexual competition in many species, although empirical data from broadcast spawners is still scant. We suggest that gamete chemoattraction could be a widespread form of female competition in sessile species. Evidence showing more intense competition in males in a majority of species (a general pattern but not a general rule) is no proof that anisogamy is the cause for that pattern. We suggest that, for example, potential reproductive rate (PRR) may be a better predictor of intrasexual competition, as it captures important ecological influences on competition. In turn, PRR may be related to gamete size in some species, if larger gametes require more time and energy to be produced, but this does not need to be the case when anisogamy initially evolves. Our results challenge the classical view that anisogamy alone is enough to explain a trend of more intense intrasexual competition in the male sex.

Appendix

Note: In the main part we present how the variables of the model are functions of the gamete traits (m_x, r_x, m_y and r_y). We will not detail this in the appendix for the sake of readability. One exception is made for the case of fertilization rates F_i and F_i' (Eqs. A9 and A14) that are used to obtain the expected evolutionary path of these gamete traits (Eqs. 4, 5, 6 in the main text). In the supplementary information S1.1 and S1.2, we give details of the mechanistic underpinning of our two mating traits (Eqs. 2-3), and below, for the fertilization dynamics.

A1 Collision frequency. To mechanistically model the fertilization dynamics between the gametes of the two mating types x and y in the mating pool, we make use of classical collision theory from chemistry and physics (McNaught et al., 2014). Hence, we assume that gametes of the two mating types x and y travel at constant speeds v_x and v_y with trajectories approximated by straight lines at a local scale. We obtain the following frequency of collisions between gametes of the two mating types (per unit of time and per unit of volume)

$$d^2\sigma_{xy}v_{xy}n_{x,t}n_{y,t}. \qquad [A1]$$

Here, $n_{i,t}$ is the number of gametes per zygote of mating type i at time t, and d is the zygote population density (number of zygotes per mating type per unit of volume). Also, $\sigma_{xy} = \pi(R_x + R_y)^2$ is the area of trajectories which would result in a collision between gametes of the two mating types, representing a disk with a radius equal to the combined radiuses of the two gametes (i.e, their collisional cross-section), assuming spherical gametes and excluding the motility machinery from the collision target. Lastly, $v_{xy} = \sqrt{v_x^2 + v_y^2}$ is the

average relative velocity between gametes of the two mating types.

A2 Gamete fertilization dynamics. Gametes of the two mating types x and y collide at a frequency given by Eq. A1 and each collision has a probability p of resulting in a fertilization event. Fertilization generates a zygote and removes the colliding gametes from the mating pool.

Multiplying Eq. A1 with p gives the fertilization rate (per unit of time and per unit of volume). Dividing the fertilization rate by the gamete density of mating type i, $d\,n_{i,t}$, gives the fertilization rate per gamete of mating type i per unit of time at time t. Multiplying this rate with the number of gametes per zygote of mating type i, $n_{i,t}$, gives the fertilization rate per zygote of mating type i per unit of time at time t.

Gametes that achieve fertilization are removed from the mating pool and the number of gametes present at time t per zygote $n_{i,t}$ therefore decreases according to their fertilization rate (negative term on the right-hand side of the equation)

$$\begin{aligned}\frac{\mathrm{d}n_{x,t}}{\mathrm{d}t} &= -pd\sigma_{xy}v_{xy}n_{x,t}n_{y,t},\\ \frac{\mathrm{d}n_{y,t}}{\mathrm{d}t} &= -pd\sigma_{xy}v_{xy}n_{x,t}n_{y,t}.\end{aligned} \tag{A2}$$

The number of gametes per zygote of the two mating types declines at the same rate ($\mathrm{d}n_{x,t}/\mathrm{d}t = \mathrm{d}n_{y,t}/\mathrm{d}t$ in Eq. A2) as each fertilization always removes one gamete of each mating type (Fisher consistent fertilization dynamics). The difference in the number of gametes between the two mating types $n_{y,t} - n_{x,t}$ thereby stays constant over the mating period and equals the initial difference $n_{y,0} - n_{x,0}$. The initial number of gametes per zygote of mating type i equals

$$n_{i,0} = n_i s_g = \frac{e(1-r_i)}{m_i}\frac{m_i - 1}{K_g + m_i - 1}, \tag{A3}$$

where n_i is the number of gametes produced per zygote of mating type i and s_g the survival probability of each gamete (see main text). Hence, the number of gametes per zygote of one mating type at time t is given by the number of gametes of the other mating type plus their initial difference,

$$n_{i,t} = n_{j,t} + n_{i,0} - n_{j,0}. \tag{A4}$$

where i is the focal mating type (x or y) and j is the other mating type.

By using the substitution in Eq. A4 we can express equation A2 as a single differential equation (as the initial gamete densities $n_{i,0}$ and $n_{j,0}$, Eq. A3, are constants)

$$\frac{\mathrm{d}n_{i,t}}{\mathrm{d}t} = -c_r n_{i,t}(n_{i,t} + n_{j,0} - n_{i,0}), \tag{A5}$$

where $c_r = pd\sigma_{xy}v_{xy}$ is a constant proportional to the fertilization rate. Eq. A5 is a separable differential equation with the following solution

$$n_{i,t} = n_{i,0}\frac{n_{j,0} - n_{i,0}}{\exp\big(c_r(n_{j,0} - n_{i,0})t\big)n_{j,0} - n_{i,0}}, \tag{A6}$$

(step-wise calculations in Supplementary information S3.1, Eq. S22).

A2.1 Gamete fertilization dynamics under isogamy. For the case of evolution under isogamic constraint, the gametes of the two mating types are constrained to equal trait values. Hence, we have that $n_{x,t} = n_{y,t}$ and the change in the number of gametes over time Eq. A5 simplifies to

$$\frac{\mathrm{d}n_{i,t}}{\mathrm{d}t} = -c_r n_{i,t}^2. \tag{A7}$$

Solving for $n_{i,t}$ in Eq. A7 gives the number of gametes per zygote of mating type i at time t under the isogamic constraint

$$n_{i,t} = \frac{n_{i,0}}{c_r n_{i,0} t + 1}. \tag{A8}$$

(step-wise calculations in Supplementary information S3.2, Eq. S23).

A3 Zygote reproductive success. When the mating period is over, the number of fertilized gametes per zygote equals $n_{i,0} - n_{i,t_{\mathrm{end}}}$ (Eqs. A3 and A6), (i.e., the number of gametes entering the mating pool subtracted by the number of unfertilized gametes at $t = t_{\mathrm{end}}$, the end of the mating period). Each fertilization produces a zygote (Fig. 3) that has a probability of survival to the next generation

of $s_z = (m_x + m_y - 1)/(K_z + m_x + m_y - 1)$ (as presented in the main text). Hence, the number of fertilized gametes per individual multiplied with the survival probability of their produced zygote s_z gives the per capita reproductive success F_i (or simply: reproductive success) corresponding to the absolute fitness of the individual,

$$F_i(T) = \Big(n_{i,0}(m_i, r_i) - n_{i,t_{\text{end}}}(T)\Big) s_z(m_i, m_j), \tag{A9}$$

where i denotes the focal mating type (x or y) and j the other mating type, and where the trait vector $T = (m_x, r_x, m_y, r_y)$ represents all four gamete traits.

A4 Fertilization dynamics of a rare mutant strategy. The strategy of a rare mutant individual $T' = (m'_x, r'_x, m'_y, r'_y)$ deviates in one or more of the four traits from the resident strategy $T = (m_x, r_x, m_y, r_y)$ (if evolution occurs under the isogamic constraint T' is replaced with $T'_{\text{c}} = (m'_{\text{c}}, r'_{\text{c}})$ and T with $T_{\text{c}} = (m_{\text{c}}, r_{\text{c}})$). The resident population is assumed to be large, and as long as the mutant strategy T' is rare its effect on the fertilization dynamics can be neglected. One can therefore consider the mutant gametes to only collide with gametes of the resident population. This is used when deriving the invasion fitness of the mutant strategy. To obtain the invasion fitness of the mutant (Eq. 4), we need its zygote reproductive success (Eq. A9), which in turn requires a solution for the gamete fertilization dynamics of the mutant (Eq. A12), given below.

A4.1 Gamete fertilization dynamics of a rare mutant strategy. Here, we derive the gamete fertilization dynamics of a rare mutant strategy. The mutant gametes are removed from the mating pool at each successful fertilization, and the number of gametes per mutant zygote $n_{i',t}$ (of mating type i at time t) decreases according to their fertilization rate (negative term on the right-hand side)

$$\frac{\mathrm{d}n_{i',t}}{\mathrm{d}t} = -pd\sigma_{i'j}v_{i'j}n_{j,t}n_{i',t}, \tag{A10}$$

where $n_{j,t}$ is the number of gametes per resident zygote of the other mating type j, $\sigma_{i'j}$ the collisional cross-section between the mutant gamete of mating type i and the resident gamete of mating type j, and $v_{i'j}$ is average relative velocity (see Appendix A1) between the mutant gamete of mating type i and the resident gamete of mating type j.

To solve for $n_{i',t}$, we first substitute the number of resident gamete $n_{j,t}$ in Eq. A10 with Eq. A6 giving

$$\frac{\mathrm{d}n_{i',t}}{\mathrm{d}t} = -\frac{c_m n_{j,0}(n_{i,0} - n_{j,0})}{\exp\Big(c_r(n_{i,0} - n_{j,0})t\Big)n_{i,0} - n_{j,0}} n_{i',t}, \tag{A11}$$

where $c_m = pd\sigma_{i'j}v_{i'j}$ is a constant proportional to the collision probability for the mutant gametes of mating type i. Eq. A11 is a separable differential equation with the following solution

$$n_{i',t} = n_{i',0}\exp(c_m n_{i,0}t)\left(\frac{n_{i,0} - n_{j,0}}{n_{i,0}\exp(c_r n_{i,0}t) - n_{j,0}\exp(c_r n_{j,0}t)}\right)^{\frac{c_m}{c_r}}, \tag{A12}$$

giving the number of unfertilized gametes per mutant zygote at time t (step-wise calculations in Supplementary information S3.3, Eq. S29).

If evolution occurs under the isogamic constraint in Eq. A10 we instead substitute the resident gamete number $n_{j,t}$ with Eq. A8 and we get

$$\frac{\mathrm{d}n_{i',t}}{\mathrm{d}t} = -\frac{c_m n_{i,0}}{c_r n_{i,0}t + 1} n_{i',t}. \tag{A13}$$

which also is a separable differential equation and has the following solution

$$n_{i',t} = n_{i',0}\left(\frac{1}{c_r n_{i,0}t + 1}\right)^{\frac{c_m}{c_r}},$$

giving the number of unfertilized gametes per mutant zygote at time t in an isogamic population (step-wise calculations in Supplementary information S3.4, Eq. S30).

A4.2 Zygote reproductive success of a rare mutant strategy. The reproductive success of a rare mutant strategy F'_i (of mating type i) follows the same logic as for the resident reproductive success (Eq. A9) and is given by

$$F'_i(m'_i, r'_i, T) = \Big(n_{i,0}(m'_i, r'_i) - n_{i',t_{\text{end}}}(m'_i, r'_i, T)\Big) s_z(m'_i, m_j), \tag{A14}$$

where i denotes the focal mating type (x or y) and j the other mating type, and where the trait vector $T = (m_x, r_x, m_y, r_y)$ gives all four gamete traits of the resident strategy.

A5 Predicting the evolutionary dynamics. Below we describe our procedure for predicting the evolutionary dynamics of the gamete traits m_x, r_x, m_y and r_y (or m_c and r_c under the isogamic constraint).

A5.1 Mutational dynamics. In our evolutionary analysis and when solving for the evolutionary path, we consider the logarithm of gamete size, $\log(m_i)$, as the evolving trait. This corresponds to mutations causing proportional changes of gamete size m_i. Similarly, we let the logit function of mating trait investment evolve $\text{logit}(r_i) = \log(r_i/[1-r])$, results in proportional changes of r_i when r_i is close to 0, or of $1 - r_i$ when r_i close to 1. For the mutation matrix C we use a scaled identity matrix, meaning that we assume no mutational covariances and equal rate of (proportional) change of the traits. By using the identity matrix scaled by one half, we get that the evolutionary path described by Eq. 6 is given by the selection gradient expressed in Eq. 5.

A5.2 Solving for isogamic singular strategies. We assume evolution to start under the isogamic constraint (where $m_x = m_y = m_c$ and $r_x = r_y = r_c$ and the isogamic strategy is given by $T_c = (m_c, r_c)$). To predict the evolutionary path (given by Eq. 6) we first numerically solve for the isogamic singular strategies T_c^*, i.e. where the selection gradient is zero, $\boldsymbol{\beta}(T_c^*) = 0$. The singular strategies represent candidates for attracting strategies. To find these isogamic singular strategies, we numerically solve for when the first and the second element of $\boldsymbol{\beta}(T_c)$ are equal to zero, separately (i.e. we solve for both isoclines). We then find their intersections, which gives the singular points.

A5.3 Stability analysis of singular strategies. To predict the evolutionary dynamics in the vicinity of a singular strategy T^* (or T_c^* under the isogamic constraint), we look at two stability properties of the singular point, namely the convergence stability and evolutionary stability. Evolutionary stability tells whether a singular strategy T^* can be invaded or not. It is uninvadable by nearby mutants if the four-dimensional Hessian matrix H of the invasion fitness (Eq. 4) with entries

$$h_{ij} = \left.\frac{\partial^2 w(T', T)}{\partial T'_i \partial T'_j}\right|_{T'=T=T^*} \qquad \text{[A15]}$$

has only negative eigenvalues, where T'_i and T'_j gives the ith and the jth element of the mutant trait vector $T' = (m'_x, r'_x, m'_y, r'_y)$. Otherwise, the singular strategy T^* is invadable by nearby mutant strategies (Leimar, 2009).

Note: if isogamic constraint is considered, replace the gamete strategies T and T' with the constraint strategies T_c and T'_c, respectively. This gives the two-dimensional Hessian matrix of the constrained evolution. The same holds for the Q-matrix and Jacobian J presented below.

Convergence stability tells whether a singular strategy T^* is an attractor or a repeller of the evolutionary path, and depends on the mutational matrix C as well as the Jacobian matrix J of the selection gradient (Eq. 5). The Jacobian, given by $\mathsf{J} = \mathsf{H} + \mathsf{Q}$ where Q is a four-dimensional square matrix with entries

$$q_{ij} = \left.\frac{\partial^2 w(T', T)}{\partial T'_i \partial T_j}\right|_{T'=T=T^*} \qquad \text{[A16]}$$

where T_j gives the jth element of the resident trait vector $T = (m_x, r_x, m_y, r_y)$)

If all eigenvalues of CJ have negative real parts, T^* is an attractor, meaning that evolution will converge towards T^*, and it is so-called convergence stable. Otherwise, it is either a saddle or a repeller of the evolutionary dynamics, meaning that evolution will diverge away from it, and we will simply refer to is as T^* being a repeller. A more stringent condition is to check if all eigenvalues of the symmetric part of the Jacobian $(\mathsf{J} + \mathsf{J}^{\mathrm{T}})/2$ have negative real parts, then T^* is so-called strongly convergence stable, meaning that it will attract for C being any matrix, not only the identity matrix (Leimar, 2009).

For two-dimensional trait-spaces, evolutionary branching can occur at singular points that have strong convergence stability and that are invadable Geritz et al., 2016. For our results, all attractors of the isogamic constraint evolution happened to have strong convergence stability, and invadability is thereby always sufficient for evolutionary branching.

For the chemoattraction mating trait, there are some extra considerations described in Supplementary information S2.2.

ACKNOWLEDGMENTS. We extend special thanks to Claus Rueffler and David Berger for their support. We also thank Ingrid Ahnesjö, Luc Bussière, Charlotta Kvarnemo, and Johanna Liljestrand Rönn for their interest in our project and helpful comments to our manuscript. We thank the editorial team of the American Naturalist and the two anonymous reviewers for a constructive review process.

Data and Code Availability

MATLAB code is available to reproduce all simulations in https://doi.org/10.5061/dryad.0rxwdbrzs.

References

Ahnesjö, I., E. Forsgren, and C. Kvarnemo. 2008. Variation in sexual selection in fishes. Enfield, NH: Science Publishers.

Almada, V. C., E. J. Gonçalves, R. F. Oliveira, and A. J. Santos. 1995. Courting females: ecological constraints affect sex roles in a natural population of the blenniid fish salaria pavo. Animal Behaviour 49:1125–1127.

Andersson, M. 1994. Sexual selection. Princeton University Press.

Bateman, A. J. 1948. Intra-sexual selection in drosophila. Heredity 2:349–368.

Beekman, M., B. Nieuwenhuis, D. Ortiz-Barrientos, and J. P. Evans. 2016. Sexual selection in hermaphrodites, sperm and broadcast spawners, plants and fungi. Philosophical Transactions of the Royal Society B: Biological Sciences 371:20150541.

Bulmer, M., and G. Parker. 2002. The evolution of anisogamy: a game-theoretic approach. Proceedings of the Royal Society of London B: Biological Sciences 269:2381–2388.

Champagnat, N., R. Ferrière, and S. Méléard. 2006. Unifying evolutionary dynamics: from individual stochastic processes to macroscopic models. Theoretical Population Biology 69:297–321.

Clutton-Brock, T. H., and G. A. Parker. 1992. Potential reproductive rates and the operation of sexual selection. The Quarterly Review of Biology 67:437–456.

Crean, A. J., and D. J. Marshall. 2008. Gamete plasticity in a broadcast spawning marine invertebrate. Proceedings of the National Academy of Sciences 105:13508–13513.

Dercole, F., and S. Rinaldi. 2008. Analysis of evolutionary processes: the adaptive dynamics approach and its applications: the adaptive dynamics approach and its applications. Princeton University Press.

Dewsbury, D. A. 2005. The darwin-bateman paradigm in historical context. Integrative and Comparative Biology 45:831–837.

Dieckmann, U., and R. Law. 1996. The dynamical theory of coevolution: a derivation from stochastic ecological processes. Journal of Mathematical Biology 34:579–612.

Durinx, M., J. A. J. H. Metz, and G. Meszéna. 2008. Adaptive dynamics for physiologically structured population models. Journal of Mathematical Biology 56:673–742.

Dusenbery, D. B. 2000. Selection for high gamete encounter rates explains the success of male and female mating types. Journal of Theoretical Biology 202:1–10.

Dusenbery, D. B. 2006. Selection for high gamete encounter rates explains the evolution of anisogamy using plausible assumptions about size relationships of swimming speed and duration. Journal of theoretical biology 241:33–38.

Dusenbery, D. B. 2009. Living at micro scale: the unexpected physics of being small. Harvard University Press.

Eisenbach, M., and L. C. Giojalas. 2006. Sperm guidance in mammals—an unpaved road to the egg. Nature reviews Molecular cell biology 7:276.

Evans, J. P., and R. A. Lymbery. 2020. Sexual selection after gamete release in broadcast spawning invertebrates. Philosophical Transactions of the Royal Society B 375:20200069.

Evans, J. P., and C. D. Sherman. 2013. Sexual selection and the evolution of egg-sperm interactions in broadcast-spawning invertebrates. The Biological Bulletin 224:166–183.

Farley, G. S., and D. R. Levitan. 2001. The role of jelly coats in sperm-egg encounters, fertilization success, and selection on egg size in broadcast spawners. The American Naturalist 157:626–636.

Forsgren, E., T. Amundsen, Å. A. Borg, and J. Bjelvenmark. 2004. Unusually dynamic sex roles in a fish. Nature 429:551.

Fromhage, L., and M. D. Jennions. 2016. Coevolution of parental investment and sexually selected traits drives sex-role divergence. Nature communications 7:1–11.

García-González, F. 2004. Infertile matings and sperm competition: the effect of "nonsperm representation" on intraspecific variation in sperm precedence patterns. The American Naturalist 164:457–472.

Geritz, S. A. H., E. Kisdi, G. Meszéna, and J. A. J. Metz. 1998. Evolutionarily singular strategies and the adaptive growth and branching of the evolutionary tree. Evolutionary Ecology 12:35–57.

Geritz, S. A. H., J. A. J. Metz, and C. Rueffler. 2016. Mutual invadability near evolutionarily singular strategies for multivariate traits, with special reference to the strongly convergence stable case. Journal of Mathematical Biology 72:1081–1099.

Gorelick, R., J. Carpinone, and L. J. Derraugh. 2017. No universal differences between female and male eukaryotes: anisogamy and asymmetrical female meiosis. Biological Journal of the Linnean Society 120:1–21.

Gowaty, P. A., Y.-K. Kim, and W. W. Anderson. 2012. No evidence of sexual selection in a repetition of bateman's classic study of drosophila melanogaster. Proceedings of the National Academy of Sciences 109:11740–11745.

Hare, R. M., and L. W. Simmons. 2018. Sexual selection and its evolutionary consequences in female animals. Biological Reviews 94.

Hoekstra, R. F. 1984. Evolution of gamete motility differences ii. interaction with the evolution of anisogamy. Journal of theoretical Biology 107:71–83.

Hoekstra, R. F., R. F. Janz, and A. Schilstra. 1984. Evolution of gamete motility differences i. relation between swimming speed and pheromonal attraction. J. theor. Biol 107:57–70.

Hoquet, T. 2020. Bateman (1948): rise and fall of a paradigm? Animal Behaviour 164:223–231.

Iyer, P., and J. Roughgarden. 2008. Gametic conflict versus contact in the evolution of anisogamy. Theoretical population biology 73:461–472.

Janicke, T., I. K. Häderer, M. J. Lajeunesse, and N. Anthes. 2016. Darwinian sex roles confirmed across the animal kingdom. Science advances 2:e1500983.

Janicke, T., and E. H. Morrow. 2018. Operational sex ratio predicts the opportunity and direction of sexual selection across animals. Ecology letters 21:384–391.

Jantzen, T., R. De Nys, and J. Havenhand. 2001. Fertilization success and the effects of sperm chemoattractants on effective egg size in marine invertebrates. Marine Biology 138:1153–1161.

Kalmus, H. 1932. Über den erhaltungswert der phänotypischen (morphologischen) anisogamie und die entstehung der ersten geschlechtsunterschiede. Biol. Zentralbl 52:716–736.

Kekäläinen, J., and J. P. Evans. 2018. Gamete-mediated mate choice: towards a more inclusive view of sexual selection. Proceedings of the Royal Society B: Biological Sciences 285:20180836.

Klochkova, T. A., T. Motomura, C. Nagasato, A. V. Klimova, and G. H. Kim. 2019. The role of egg flagella in the settlement and development of zygotes in two saccharina species. Phycologia 58:1–9.

Kokko, H., and M. D. Jennions. 2008. Parental investment, sexual selection and sex ratios. Journal of evolutionary biology 21:919–948.

Kokko, H., M. D. Jennions, and R. Brooks. 2006. Unifying and testing models of sexual selection. Annu. Rev. Ecol. Evol. Syst. 37:43–66.

Kokko, H., H. Klug, and M. D. Jennions. 2012. Unifying cornerstones of sexual selection: operational sex ratio, bateman gradient and the scope for competitive investment. Ecology Letters 15:1340–1351.

Kvarnemo, C., and I. Ahnesjo. 1996. The dynamics of operational sex ratios and competition for mates. Trends in Ecology & Evolution 11:404–408.

Lehtonen, J., and H. Kokko. 2011. Two roads to two sexes: unifying gamete competition and gamete limitation in a single model of anisogamy evolution. Behavioral ecology and sociobiology 65:445–459.

Lehtonen, J., and G. A. Parker. 2014. Gamete competition, gamete limitation, and the evolution of the two sexes. Molecular human reproduction 20:1161–1168.

Lehtonen, J., G. A. Parker, and L. Schärer. 2016. Why anisogamy drives ancestral sex roles. Evolution 70:1129–1135.

Leimar, O. 2009. Multidimensional convergence stability. Evolutionary Ecology Research 11:191–208.

Lessells, C., R. Snook, and D. Hosken. 2009. The evolutionary origin and maintenance of sperm: selection for a small, motile gamete mating type. Pages 43–67 *in* Sperm Biology: An Evolutionary Perspective. Elsevier.

Levitan, D. R. 1993. The importance of sperm limitation to the evolution of egg size in marine invertebrates. The American Naturalist 141:517–536.

Levitan, D. R. 1996. Effects of gamete traits on fertilization in the sea and the evolution of sexual dimorphism. Nature 382:153.

Levitan, D. R. 1998*a*. Does bateman's principle apply to broadcast-spawning organisms? egg traits influence in situ fertilization rates among congeneric sea urchins. Evolution 52:1043–1056.

Levitan, D. R. 1998*b*. Sperm Limitation, Gamete Competition, and Sexual Selection in External Fertilizers. Elsevier.

Levitan, D. R. 2004. Density-dependent sexual selection in external fertilizers: variances in male and female fertilization success along the continuum from sperm limitation to sexual conflict in the sea urchin strongylocentrotus franciscanus. The American Naturalist 164:298–309.

Levitan, D. R., and C. Petersen. 1995. Sperm limitation in the sea. Trends in Ecology & Evolution 10:228–231.

Lüpold, S., and J. L. Fitzpatrick. 2015. Sperm number trumps sperm size in mammalian ejaculate evolution. Proc. R. Soc. B 282:20152122.

Marshall, D., and J. Evans. 2005. Does egg competition occur in marine broadcast-spawners? Journal of evolutionary biology 18:1244–1252.

McNaught, A. D., A. Wilkinson, M. Nic, J. Jirat, and B. Kosata. 2014. IUPAC Compendium of Chemical Terminology, 2nd ed. (the "Golden Book") on-line corrected version, vol. 1669. Oxford, Blackwell Scientific Publications.

Metz, J. A. J., and C. G. F. de Kovel. 2013. The canonical equation of adaptive dynamics for Mendelian diploids and haplo-diploids. Interface Focus 3.

Metz, J. A. J., R. M. Nisbet, and S. A. H. Geritz. 1992. How should we define 'fitness' for general ecological scenarios? Trends in Ecology & Evolution 7:198–202.

Milner-Gulland, E., O. Bukreeva, T. Coulson, A. Lushchekina, M. Kholodova, A. Bekenov, and I. A. Grachev. 2003. Conservation: Reproductive collapse in saiga antelope harems. Nature 422:135.

Morrow, E. H. 2004. How the sperm lost its tail: the evolution of aflagellate sperm. Biological Reviews 79:795–814.

Motomura, T., and Y. Sakai. 1988. The occurrence of flagellated eggs in laminaria angustata (phaeophyta, laminariales) 1. Journal of phycology 24:282–285.

Niemeyer, C. L., and J. R. Anderson. 1983. Primate harassment of matings. Ethology and Sociobiology 4:205–220.

Parker, G. A. 1982. Why are there so many tiny sperm? sperm competition and the maintenance of two sexes. Journal of theoretical biology 96:281–294.

Parker, G. A. 2014. The sexual cascade and the rise of pre-ejaculatory (darwinian) sexual selection, sex roles, and sexual conflict. Cold Spring Harbor perspectives in biology 6:a017509.

Parker, G. A., R. R. Baker, and V. Smith. 1972. The origin and evolution of gamete dimorphism and the male-female phenomenon. Journal of theoretical biology 36:529–553.

Parker, G. A., and T. Pizzari. 2015. Sexual selection: the logical imperative. Pages 119–163 *in* Current perspectives on sexual selection. Springer.

Podolsky, R. D. 2002. Fertilization ecology of egg coats: physical versus chemical contributions to fertilization success of free-spawned eggs. Journal of Experimental Biology 205:1657–1668.

Priklopil, T., and L. Lehmann. 2020. Invasion implies substitution in ecological communities with class-structured populations. Theoretical population biology 134:36–52.

Queller, D. C. 1997. Why do females care more than males? Proceedings of the Royal Society of London B: Biological Sciences 264:1555–1557.

Schärer, L., L. Rowe, and G. Arnqvist. 2012. Anisogamy, chance and the evolution of sex roles. Trends in Ecology & Evolution 27:260–264.

Seed, C. E., and J. L. Tomkins. 2018. Positive size–speed relationships in gametes and vegetative cells of chlamydomonas reinhardtii; implications for the evolution of sperm. Evolution 72:440–452.

Shaw, R. F., and J. D. Mohler. 1953. The selective significance of the sex ratio. The American Naturalist 87:337–342.

Singh, A., and D. Punzalan. 2018. The strength of sex-specific selection in the wild. Evolution 72:2818–2824.

Sutherland, W. J. 1985. Chance can produce a sex difference in variance in mating success and explain bateman's data. Animal Behaviour 33:1349–1352.

Tang-Martinez, Z., and T. B. Ryder. 2005. The problem with paradigms: Bateman's worldview as a case study. Integrative and Comparative Biology 45:821–830.

Togashi, T., T. Motomura, and T. Ichimura. 1997. Production of anisogametes and gamete motility dimorphism in monostroma angicava. Sexual Plant Reproduction 10:261–268.

Togashi, T., Y. Sakisaka, T. Miyazaki, M. Nagisa, N. Nakagiri, J. Yoshimura, K.-i. Tainaka, P. A. Cox, and J. L. Bartelt. 2009. Evolution of gamete size in primitive taxa without mating types. Population ecology 51:83–88.

Van Dooren, T. J., M. Durinx, and I. Demon. 2004. Sexual dimorphism or evolutionary branching? Evolutionary Ecology Research 6:857–871.

Yund, P. O. 2000. How severe is sperm limitation in natural populations of marine free-spawners? Trends in Ecology & Evolution 15:10–13.

Supplementary Information to: Anisogamy Does Not Always Promote the Evolution of Mating Competition Traits in Males

Mattias Siljestam[1] **and Ivain Martinossi-Allibert**[2,*]

[1] Department of Ecology and Genetics, Animal Ecology, Uppsala University, Norbyvägen 18D, 752 36 Uppsala, Sweden

[2] Department of Biology, Norwegian University of Science and Technology NTNU, 7491 Trondheim, Norway

[*] To whom correspondence should be addressed. E-mail: imartinossi@gmail.com

ORCIDs: Siljestam, https://orcid.org/0000-0002-3720-4926; Martinossi-Allibert, https://orcid.org/0000-0002-8332-8620

S1. Model

S1.1 Fluid dynamics of gametes locomotion. In our first scenario, we consider a flagella-like mating trait, allowing the gamete to move and encounter a fusion partner. Below, we use fluid dynamics to derive an equation of the speed of the gamete as a function of its size and energy spent on the trait.

For small entities (< 1mm) moving in water, viscosity is the dominating force and the effects of inertia can be neglected (this corresponds to low Reynolds numbers, Dusenbery, 2009). Under such circumstances, Stoke's law applies, giving the frictional force F_f for a small sphere moving through still water

$$F_f = 6\pi\eta R v, \tag{S1}$$

which is linearly dependent on the viscosity of the water η, the radius of the sphere R, and the speed at which the sphere moves v (Dusenbery, 2009).

A gamete with a constant thrust will, due to its small size resulting in small Reynolds number, reach its equilibrium speed quickly. At equilibrium speed, the force of propulsion is equal to the frictional force $F_p = F_f$. Applying this to Stokes law (Eq. S1) gives us the gamete speed at this equilibrium

$$v = \frac{F_p}{6\pi\eta R}. \tag{S2}$$

Hence, to derive the gamete speed at equilibrium we need the viscosity of the water η, which is a constant, the radius of the gamete R, and the force that propels the gamete at equilibrium F_p. To obtain F_p, we rely on the methods proposed by Dusenbery (2009), giving two different approaches which result in two different size-speed relationships: one in which speed is proportional to size, and one in which speed is inversely proportional to size.

Speed proportional to size. In this first path of derivation, we assume that a gamete of volume m has a total metabolism M proportional to its volume: $M = c_M m$, with c_M giving the proportional relationship between these. Out of the total metabolism M, a certain proportion is dedicated to the propulsion $M_p = c_p M$, and the remaining proportion is dedicated to base metabolism $M_b = (1 - c_p)M$. The metabolism dedicated to propulsion M_p has an energy conversion efficiency of c_e to realized propulsion power, and the power of the propulsion P_p is therefore given by $P_p = c_e M_p = c_e c_p M = c_e c_p c_M m$. Hence, the power of propulsion is proportional to the volume of the gamete m. As power, force and velocity have the following relationship $P = Fv$, we get that $F_p = P_p/v$ and plugging this into Eq. S2,

together with the volume to radius relationship of a sphere $m = (4\pi/3)R^3$, gives

$$v = \frac{P_p}{6\pi\eta R v} \iff$$
$$v = \sqrt{\frac{2c_e c_p c_M}{9\eta}} R \qquad [S3]$$

where the equilibrium gamete speed v is proportional to its linear size (radius) R of the gamete, and everything within the square root determines this linear relationship. There is good empirical evidence for such a linear size-speed relationship when comparing the motility of small organisms in water across a large range of genera of different sizes (Dusenbery, 2009, Fig. 8.3), as well as comparing gamete speeds between genus (Dusenbery, 2009, Table 20.1).

In our model, m gives the energy spent per gamete on gamete volume (and we let one unit of energy convert into one unit of volume, and therefore m also gives the gamete volume), while $mr/(1-r)$ gives the energy spent per gamete on the gamete motility trait. We let the base metabolism M_b and the metabolism dedicated to the propulsion M_p be proportional to the energy spent on gamete volume m and the energy spent on the propulsion trait $r/(1-r)m$, respectively. We let the constant $\hat{c}_M$ determine these relationships such that $M_b = \hat{c}_M m$ and $M_p = \hat{c}_M mr/(1-r)$. The total metabolism M is therefore given by $M = \hat{c}_M m/(1-r) = c_M m$, and we get that $c_M = \hat{c}_M/(1-r)$. Hence, the metabolism per gamete volume c_M is an increasing function of r, where a gamete investing a lot of energy into locomotion will simply have a higher overall metabolism per gamete volume.

We find that the proportion of metabolism dedicated to propulsion c_p (given by M_p/M), equals the proportion of energy invested into propulsion, i.e. $c_p = r$. Plugging this into Eq. S3 gives

$$v = c_{v1}\sqrt{\frac{r}{1-r}} R, \qquad [S4]$$

where $c_{v1} = \sqrt{\frac{2c_e\hat{c}_M}{9\eta}}$ encompasses the remaining constants and $r/(1-r)$ gives the energy spent on locomotion relative to the energy spent on gamete mass.

To summarize, we find that gamete speed is proportional to linear size R, and is also an increasing function of the proportion of energy invested into propulsion r.

Speed inversely proportional to size. This second approach has a less mechanistic underpinning, but is based on insights from empirical evidence comparing gamete speeds within genera, suggesting that it may be more appropriate to assume the force of propulsion F_p to be invariant to cell size (Dusenbery, 2009, Table 20.1). Assuming F_p to be constant leads to gamete speed being inversely proportional to gamete radius: $v \propto R^{-1}$ (Eq. S2), which is the classically assumed scenario for earlier mechanistic models of anisogamy evolution (Hoekstra, 1984; Hoekstra et al., 1984; Dusenbery, 2000, 2006; Togashi et al., 2009).

In our model, $r/(1-r)$ gives the energy spent on the locomotion machinery relative to the rest of the gamete. So, even if F_p is assumed to be invariant to size, we let it depend on $r/(1-r)$ such that: $F_p = c_F[r/(1-r)]^{\alpha_r}$, where $\alpha_r = 1$ gives a linear relationship between investment in locomotion and the force of propulsion, $\alpha_r < 1$ gives a diminishing rate of return and $\alpha_r > 1$ an increasing rate of return. Plugging this into Eq. S2 gives

$$v = c_{v2}\left(\frac{r}{1-r}\right)^{\alpha_r} R^{-1}, \qquad [S5]$$

where $c_{v2} = c_F/(6\pi\eta)$ encompasses all the constants, and gives an equation similar to Eq. S4, but with gamete speed being proportional to the inverse of the linear size.

Combining both size-speed relationships. These two approaches results in equations with opposite behaviour in terms of the size-speed relationships (Eqs. S4 and S5), but both relationships have empirical support. As mentioned above, the positive size-speed relationship has empirical support across genera, while the inverse size-speed relationship has empirical support for within genera (Dusenbery, 2009, Fig. 8.3 and Table 20.1). This leaves us with two different size-speed relationships that are relevant to consider. For Eq. S5 we found that α_r did not have any strong effects on the outcome, and with inspiration from the appearance of Eq. S4 we chose to stick with $\alpha_r = 1/2$ for practicality, as both Eq. S4 and S5 can then be expressed by the following

$$v = c_{v3}\sqrt{\frac{r}{1-r}}R^{\alpha_m}, \tag{S6}$$

where c_{v3} is a constant scale factor. Setting $\alpha_m = 1$ gives Eq. S4 (with $c_{v3} = c_{v1}$) and $\alpha_m = -1$ gives Eq. S5 (with $c_{v3} = c_{v2}$), and an intermediate value of α_m corresponds to an intermediate scenario

Given the radius-volume relationship of a sphere $R = (6m/\pi)^{1/3}/2$, we can write Eq. S6 as a function of gamete volume m, as well as mating trait investment r, such that the gamete speed of a gamete of mating type i is given by

$$v_i(m_i, r_i) = v_0\sqrt{\frac{r_i}{1-r_i}}m_i^{\alpha_m/3}, \tag{S7}$$

where v_0 is a constant scale factor encapsulating all constants: $v_0 = c_{v3}(6/\pi)^{1/3}/2$.

S1.2 Gamete fusion partner capture. In the second scenario of the model, we introduce another mating trait that increases the collision target size of the gamete. Gametes move around randomly, with similar motility v_0, which is invariant to size, and the mating trait either increases the gamete target size through physical structures or by chemoattraction. In the absence of this trait, the gamete volume m is made of the expensive vital structures, increasing the survival probability of both the gamete and its potential zygote. The cost to produce this vital gamete volume is assumed to be proportional to its volume m (where we assume, without loss of generality, that one unit of energy produces one unit of gamete volume).

The mating trait introduces a less costly way of increasing the collision target, without giving any benefits in terms of survival of the gamete or zygote. The efficiency of this mating trait depends on the dimensionality of the scaling between energy invested and increase in apparent size. We take different variations into account, including both physical structures and chemoattraction.

Physical structures. First, the gamete can increase its apparent volume by producing a jelly coat, which is cheaper than the volume of the gamete cell. With the cost of producing one unit of volume of jelly c_J, as well as the energy spent on the mating trait $mr/(1-r)$, we get the following volume of the gamete's collision target $\hat{m} = m + (1/c_\mathrm{J})mr/(1-r)$, where m gives the volume of the gamete without the mating trait. This can be rewritten as

$$\hat{m} = m\left(1 + \alpha_r\frac{r}{1-r}\right), \tag{S8}$$

where $\alpha_r = 1/c_\mathrm{J}$ encompasses the constants. For the jelly coat to be cheaper to produce than the vital gamete volume, α_r must be greater than 1.

Second, the gamete can increase its apparent volume $\hat{m}$ by filling the cell with cytoplasm and producing a corresponding amount of extra cell membrane surface to encapsulate this additional volume. Here, we assume that the cytoplasm has a negligible cost in comparison to the cell membrane, which has a cost of c_M per unit of membrane surface area. This gives a surface area of the gamete collision target of $\hat{A} = A + (1/c_\mathrm{M})mr/(1-r)$, where A is the surface area the cell would have without the mating trait. With the relationships between volume m and surface area A of a sphere, with $m = A^{3/2}/(6\sqrt{\pi})$ and therefore $A = (6\sqrt{\pi}m)^{2/3}$, we get that the total volume of the

gamete $\hat{m}$ is given by

$$\hat{m} = m\left(1 + \alpha_r m^{1/3}\frac{r}{1-r}\right)^{3/2}, \quad [S9]$$

where $\alpha_r = 1/[(6\sqrt{\pi})^{2/3} c_{\mathrm{M}}]$ encompasses the constants. We assume, in turn, that the cell membrane is cheap to produce in comparison to producing the vital gamete volume (e.g., the membrane cost is neglected in the cost of producing the main volume of the cell m, being proportional to volume only). For the minimum cell volume of $m = 1$, there are $(6\sqrt{\pi})^{2/3} \approx 5$ units of area per unit of volume of a sphere (this drops to around 1 at $m = 100$, and around 1/5 at $m = 10^4$), and the cost of the membrane c_{M} must be much smaller than 1/5 for the membrane to have a negligible cost compared to vital cell mass. This corresponds to $\alpha_r >> 1$.

To provide a comprehensive analysis, we include a third variation of this mating trait, lacking a biological example. Similar to the second, the gamete can increase its apparent volume by filling the cell with cheap cytoplasm and extending its membrane correspondingly, but there is also a requirement to generate a cellular function (or structure) for which the cost scales with the radius of the cell. In this third scenario, we assume the cost of both the cytoplasm and membrane to be negligible compared to this cellular function, and c_{F} gives the cost of this cellular function associated with increasing the cell radius by one unit of length. Hence, the gamete's total radius is given by $\hat{R} = R + (1/c_{\mathrm{F}})mr/(1-r)$. Using the volume-radius relationships of a sphere, we express the total volume of the gamete as

$$\hat{m} = m\left(1 + \alpha_r m^{2/3}\frac{r}{1-r}\right)^{3} \quad [S10]$$

where $\alpha_r = (4\pi/3)^{1/3}/c_{\mathrm{F}}$ encompasses the constant.

We assume, in turn, that this cellular function is cheap to produce in comparison to the vital gamete volume. For the minimum cell volume of $m = 1$, the radius per unit of volume is $[3/(4\pi)]^{1/3} \approx 0.62$ (this drops quickly, to 0.13 at $m = 10$, and 0.003 at $m = 100$), and the cost of this cellular function c_{F} must be much smaller than 1/0.62 for the membrane to have a negligible cost compared to vital cell mass. This corresponds to $\alpha_r >> 1$.

Combining all three cost-size relationships. The three variations of physical traits increasing the collision target of the gamete, expressed in Eqs. S8, S9 and S10, can be summarized by the following single equation where the volume of the collision target of a gamete of mating type i is given by

$$\hat{m}_i(m_i, r_i) = m_i\left(1 + \alpha_r m_i^{(3-\alpha_d)/3}\frac{r_i}{1-r_i}\right)^{3/\alpha_d}. \quad [S11]$$

Here, the parameter α_d gives the dimensionality at which the mating trait scales with energy investment, where for a jelly coat the energy investment scales with the increased volume ($\alpha_d = 3$), for the membrane with the increased surface area ($\alpha_d = 2$) and for the last case with the increased radius ($\alpha_d = 1$). As motivated above, we assume that α_r, giving how efficient the mating trait is, should be greater than 1 for all these three trait variations. We investigate the model for $\alpha_r = 10$.

Chemoattraction. As an alternative to the scenario above, where the gamete uses physical structures to increase its collision target, we also consider a scenario where gametes can use chemoattraction to attract a fusion partner. In this case, the gametes of both mating types produce and release chemoattractants, which gametes of the other mating type can detect at a certain threshold concentration C_d (being equal for both mating types). At detection, fertilization ensues at probability p.

Chemicals in still water spread through diffusion. We model all chemical releases as point sources at the centre of the gametes. A point source releasing chemicals at a steady rate J will reach a diffusion equilibrium with the concentration C at distance R_c given by

$$C = \frac{J}{4\pi D R}, \quad [S12]$$

where D is the diffusion constant of water. For the chemoattraction scenario, we assume low gamete speed (small v_0) such that the

equilibrium concentration in Eq. S12 is reached quickly around a gamete, in comparison to their slow movement. At the same time, we assume a correspondingly longer mating period ($t_{\max}$), such that the relevant parameter $\delta \propto v_0 t_{\max}$ is unaffected.

A gamete has a natural constant release rate J_n of the chemoattractant, resulting in the detectable concentration level C_d at their surface such that the fertilization behaviour activates on contact. Eq. S12 then gives $J_n = 4\pi DRC_d$. The gamete can spend extra energy to increase the release rate of the chemoattractant by J_a over the mating period, and thereby enlarging the radius of detection. The increased release rate is proportional to the energy spent: $J_a = (1/c_a)mr/(1-r)$, where c_a gives the cost of increasing the release rate by one unit. The concentration of the attractant C_a at distance R_a from the centre point of the gamete is then given by

$$C_a = C_d + m\frac{r}{1-r}\frac{1}{4\pi DR_a c_a}.$$

The gamete can be detected at the distance where $C_a = C_d$, and the extended radius of detection gained from the chemoattractant equals $\Delta R = (1/c_c)mr/(1-r)$, where $c_c = 4\pi DC_d c_a$ encompasses the constants. In contrast to the physical traits presented above, the benefits of chemoattractant does not add between the two mating types: as soon as the gamete with the larger chemoattractant zone triggers fertilization, the smaller chemoattractant zone of the other gamete is redundant. This means that the radius of a gamete's effective collision target (including the increase from the chemoattractant) is simply given by R_i (no increase) for the mating type with the smaller chemoattractant zone and $R_i + \Delta R_i = R_i + (1/c_c)mr/(1-r)$ for the mating type with the larger chemoattractant zone (which happens to be the same expression as for the cellular functions scaling with the radius, $\alpha_d = 1$, above).

Using the volume-radius relationships of a sphere, the apparent volume of the gamete with the larger chemoattractant zone is given by

$$\hat{m}_L(m_i, r_i) = m_i\left(1 + \alpha_r m_i^{2/3}\frac{r_i}{1-r_i}\right)^3 \qquad \text{[S13]}$$

where $\alpha_r = 1/[(48\pi^2)^{1/3}DC_d c_a]$ encompasses the constant (note that this equation equals Eq. S11 for $\alpha = 1$). And simply $\hat{m}_i(m_i) = m_j$ if it is the mating type with the smaller chemoattractant zone (i.e., the mating trait investment r_j has no effect).

The radius of the effective collisional cross-section between two gametes is given by $R_i + R_j + \Delta R_i$, where $i \in \{x, y\}$ is the mating type with the larger chemoattractant zone, and under isogamy (or any other trait combination resulting in equal chemoattractant zone) this equals $2R_= + \Delta R_=$, as the chemoattractant zones are of equal size $\Delta R_x = \Delta R_y = \Delta R_=$ (even though the same benefit would be gained from only one using the chemoattractant). The radius of a gamete's effective collision target is therefore given by $R_= + \Delta R_=/2 = R_i + 1/(2c_c)mr/(1-r)$.

The general equation for the apparent volume, encompassing all three situations (larger, smaller or equal chemoattractant zone), is then given by

$$\hat{m}_i(m_i, r_i) = \begin{cases} \hat{m}_L(m_i, r_i), & \text{if } \hat{m}_L(m_i, r_i) > \hat{m}_L(m_j, r_j) \\ m_i, & \text{if } \hat{m}_L(m_i, r_i) < \hat{m}_L(m_j, r_j) \\ \frac{\hat{m}_L(m_i, r_i) + m_i}{2}, & \text{if } \hat{m}_L(m_i, r_i) = \hat{m}_L(m_j, r_j), \end{cases} \qquad \text{[S14]}$$

where $\hat{m}_L$ refers to Eq. S13.

Under isogamic constraint, the apparent volume is always given by the third case of equal sized chemoattractant zones ($\hat{m}_L(m_i, r_i) = \hat{m}_L(m_j, r_j)$) which equals

$$\hat{m}_{\mathrm{c}}(m_{\mathrm{c}}, r_{\mathrm{c}}) = m_{\mathrm{c}}\left(1 + \frac{1}{2}\alpha_r m_{\mathrm{c}}^{2/3}\frac{r_{\mathrm{c}}}{1-r_{\mathrm{c}}}\right)^3. \qquad \text{[S15]}$$

S2. Analysis

S2.1 Symmetries of the invasion fitness function. In our model, the fertilization dynamics of the two mating types x and y are modelled identically, such that the label x and y have no effect *per se*. This symmetry means that, for a resident trait vector $T = (m_i, r_i, m_j, r_j)$ and an alternative trait vector $T_{\text{rev}} = (m_j, r_j, m_i, r_i)$ where the two mating types are reversed, we have $F_i'(m', r', T) = F_j'(m', r', T_{\text{rev}})$ for the mutant (and correspondingly $F_i(T) = F_j(T_{\text{rev}})$ for the resident). Here i denotes either mating type x or y, and j denotes the other mating type. We refer in several instances to the work of Van Dooren et al. (2004), where another type of symmetry is considered and should not be confused with what we present in our model. Van Dooren et al. (2004) consider $F_x(m', r', T) = F_y(m', r', T) = F(m', r', T)$, meaning that a male and a female of the same phenotype have the same reproductive success. In our model, the reproductive success of each mating type (or sexes if anisogamy evolves) depends on the fertilisation dynamics. A given phenotype is likely to result in different reproductive successes in males and females if anisogamy has evolved.

The two types of symmetries result in some similarities between the models. For an isogamic population (without the isogamic constraint) with the strategy $T_= = (m, r, m, r)$, a mutant has the same reproductive success irrespective of its mating type: $F_x(m', r', T_=) = F_y(m', r', T_=) = F_=(m', r', T_=)$, which equals the reproductive success under the isogamic constraint $F_=(m', r', T_=) = F_{\text{c}}(m', r', T_{\text{c}})$, where $T_{\text{c}} = (m, r)$.

Hence, the partial derivatives with the respect to mutant traits are the same for F_{c} and $F_=$, and each singular strategy of the constraint trait space T_{c}^* is therefore also a singular strategy at its corresponding point in the unconstrained trait space $T_=^*$. In addition, as the Hessian (Eq. A15) only takes partial derivatives with respect to the mutant traits, the Hessian of the unconstrained evolution $\mathsf{H}(\mathsf{T}_=^*)$ is a 4×4 block diagonal matrix, with the 2×2 Hessian of the constrained evolution $\boldsymbol{H}(T_{\text{c}}^*)/2$ at its diagonal, and zero matrices at the off-diagonal (Van Dooren et al., 2004),

$$\mathsf{H}(\mathsf{T}_=^*) = \frac{1}{2}\begin{pmatrix} \mathsf{H}(T_{\text{c}}^*) & \mathbf{0} \\ \mathbf{0} & \mathsf{H}(T_{\text{c}}^*). \end{pmatrix}$$

However, the two types of symmetries found in our model and in Van Dooren et al. (2004) results in different properties of the Jacobian (and the Q-matrix, Eq. A16) evaluated at an isogamic strategy $T_=$.

In Van Dooren et al. (2004), at a strategy without differentiated mating types (isogamy in our model), both the eigenvalues of the Hessian H_{c} and Jacobian J_{c} for the constrained evolution, divided by two, appear as eigenvalues of the Jacobian for the unconstrained evolution $J_=$. In our model, only the eigenvalues of J_{c}, divided by two, appear as eigenvalues of $\mathsf{J}_=$.

In summary, for both models, an isogamic singular point that is repelling for the isogamic constrained evolution (J_{c} having positive eigenvalues) always coincides with the singular point repelling the unconstrained evolution ($\mathsf{J}_=$ having positive eigenvalues). However, only in the model of Van Dooren et al. (2004) is there a link between the singular point repelling ($\mathsf{J}_=$ having positive eigenvalues) and invadability of the singular point under the constrained evolution (H_{c} having positive eigenvalues). This is not the case in our model, and we can therefore find singular points of the constrained evolution that can only transition into anisogamy, without having the possibility of transitioning into genetic polymorphism instead (see scenario (2) in the Analysis section).

S2.2 Stability analysis for chemoattraction. The mating trait of chemoattraction is modelled by a symmetric but non-smooth function for unconstrained evolution (Eq. S14), as the trait is only effective for the mating type with the larger chemoattraction zone having an apparent volume given by Eq. S13. The function (Eq. S14) is therefore undifferentiable at any point where chemoattraction zones are equal for both mating types, which includes all the isogamic points. In contrast, for the isogamic constraint case the function is smooth, and the apparent volume is always given by the one case of equal sized chemoattractant zones, Eq S15.

We do know, however, that all the isogamic unconstrained singular point $T*_{=}$ where $r_c > 0$ are repeller. As soon as the smallest divergence in the trait of the two mating types occurs, the mating type that happens to get the smaller chemoattraction zone will always get a negative selection gradient of r_j (we arbitrarily label this mating type j). This happens because the investment into the mating trait gives no benefit for the mating type with the smaller attraction radius, but decreases gamete numbers in Eq. 1 and thus r_j will always evolve to zero. Therefore, only points $T*_{=}$ where $r_c = 0$ can be attractors.

To overcome the problem of undifferentiability, we model the mating trait of chemoattraction by smooth functions that are asymmetrical between the mating types, by simply not considering the possibility of mating type j switching from having the small to the larger chemoattractant zone. This means that

$$\begin{cases} \hat{m}_i(m_i, r_i) & = \hat{m}_L(m_i, r_i), \\ \hat{m}_j(m_j) & = m_j, \end{cases} \qquad \text{[S16]}$$

where $\hat{m}_L$ is given in Eq. S13 above.

When the model is expressed by this function, the model is no longer symmetric between the mating types, and the result from the section above that a unconstrained strategy $T^*_=$ corresponding to a singular point in the constrained trait space T^*_c is a singular point in the unconstrained space as well, does not hold any more.

In practice, some of the isogamic singular points that are repelling for the unconstrained evolution for the original symmetric function (Eq. S14), will just appear as points with non-zero selection gradient β for the smooth function (Eq. S16, e.g. when $r_c > 0$. However, for both functions the behaviour is then the same: evolution leads away from $T^*_=$ in the same way, and $T^*_=$ is considered a repeller.

On the other hand, if $T^*_=$ happens to be a singular point with the smooth function, we just use the methods presented in Appendix A5.3 to see if it is an attractor or repeller of the evolutionary dynamics.

S2.3 Numerically solving for the evolutionary path. As a complement to the stability analysis, we numerically solve for the evolutionary path given by Eq. 6 using the Runge-Kutta method with adaptive step size of order 4 and 5.

First, we solve for the evolutionary path under the isogamic constraint. As there is always a single attracting strategy for the parameter range we investigate (see Analysis section), the starting point has no particular meaning, and we start evolution from an arbitrary point chosen to be $T_c = (m_c = 100, r_c = 10^{-5})$. We continue the evolutionary path until the evolutionary equilibrium is reached at an attractor $T^a_c = (m^a_c, r^a_c)$. Then, we continue the evolution without the isogamic constraint with a small initial divergence ϵ in either gamete size m or mating trait investment r between the two mating types, such that $T = (m^a_c + \epsilon, r^a_c, m^a_c - \epsilon, r^a_c)$ or $T = (m^a_c, r^a_c + \epsilon, m^a_c, r^a_c - \epsilon)$. If evolution in both cases leads back towards $T = (m^a_c, r^a_c, m^a_c, r^a_c)$, we conclude that the isogamic attractor T^a_c is also an attractor of the corresponding unconstrained evolution. In this case, there is stabilizing selection preventing the evolution of anisogamy and the isogamic attractor T^a_c is the end-point of evolution. Otherwise, if the trait values of the two mating types diverge away from T^a_c, it is a repeller of the unconstrained evolution and anisogamy evolves. We then continue the numerical solution of the evolutionary path until anisogamic evolution reaches an attractor, most often it is a fixed point attractor $T^a = (m^a_x, r^a_x, m^a_y, r^a_y)$ giving an evolutionary endpoint (see Fig. 4b-c), but for a small subset of the parameter values it reaches a limit cycle attractor, resulting in stable oscillations (see Fig. 4d).

S2.4 Partial derivatives on fitness. In this part, we connect predictions of the model to partial derivatives of the invasion fitness w (Eq. 4) with respect to a mutant trait. This complements the verbal arguments made in the main part, giving a better understanding of how the evolving traits of the model (m_x, r_x, m_y and r_y) affect the trade-offs between the three fitness components: gamete numbers $n_{i,0}$, fertilization success f_i and zygote survival s_z. The partial derivatives of the invasion fitness w with respect to the four gamete traits make up β in Eq. 6, where a positive partial derivative means that a mutant with a higher value of that trait can invade, and *vice versa*. The partial derivative of the invasion fitness w with respect to the mutant trait of mating type i is proportional to the corresponding partial derivative of the reproductive success F_i' (i.e., $\partial w/\partial r_i' \propto \partial F_i'/\partial r_i'$), and as we are only interested in the sign of the expression, we can look at the derivative of F_i' instead.

The reproductive success F_i can be expressed as the product of three fitness components: $F_i = n_{i,0} f_i s_z$, i.e., the number of gametes entering the mating pool times their fertilization success times their zygote survival probability. The partial derivative of the mutant fertilization success F_i' with respect to the mating trait investment r_i' gives

$$\frac{\partial F_i'}{\partial r_i'} = \frac{\partial f_i' n_{i',0} s_z'}{\partial r_i'} = f_i' s_z' \frac{\partial n_{i',0}}{\partial r_i'} + n_{i',0} s_z' \frac{\partial f_i'}{\partial r_i'} + n_{i',0} f_i' \frac{\partial s_z'}{\partial r_i'}.$$

We know the signs of all these three derivatives, as the investment into the mating trait has only two effects. First, r_i increases the mating trait (gamete motility or apparent gamete size) which, per definition, increases fertilization success f_i. Second, investing energy imposes a traded-off, as spending the proportion r_i of energy on the mating trait decreases the gamete numbers accordingly. Finally, r_i has no effect on zygote survival. In conclusion, $\partial n_{i',0}/\partial r_i' < 0$, $\partial f_i'/\partial r_i' > 0$ and $\partial s_z'/\partial r_i' = 0$, and

$$\frac{\partial F_i'}{\partial r_i'} = f_i' s_z' \frac{\partial n_{i',0}}{\partial r_i'} + n_{i',0} s_z' \frac{\partial f_i'}{\partial r_i'},$$

and the mating trait evolves whenever the increase in fertilization success f_i' outweighs the decrease in gamete numbers $n_{i,0}'$. Under the special case of complete absence of gamete limitation (classically referred to as *gamete competition*), the fertilization success of female gametes $f_x = 1$ and can not be increased. Therefore, independently of how effective the mating trait is, $\partial f_x'/\partial r_x' = 0$ and r_x will not evolve. Otherwise, if $f_x < 1$, both mating types can evolve the mating trait, as seen in the results of our model (Figures 5, S1 and S2).

For gamete size m_i, we have

$$\frac{\partial F_i'}{\partial m_i'} = \frac{\partial f_i' n_{i',0} s_z'}{\partial m_i'} = f_i' s_z' \frac{\partial n_{i',0}}{\partial m_i'} + n_{i',0} s_z' \frac{\partial f_i'}{\partial m_i'} + n_{i',0} f_i' \frac{\partial s_z'}{\partial m_i'},$$

where zygote survival is an increasing function of m_i (i.e., $\partial s_z/\partial m_i > 0$), while for the gamete number $n_{i,0}$ there is an intermediate optimum of $m_i = \sqrt{K_g} + 1$, and the sign of $\partial n_{i,0}/\partial m_i$ will depend on whether m_i is greater than or smaller than this. The sign of $\partial f_i'/\partial m_i'$ will depend on the mating trait: it is positive for the fusion partner capture trait (increasing apparent size), and for the gamete motility trait whenever $\alpha_m > 0$. It is negative whenever $\alpha_m < 0$ for the gamete motility trait. The sign of the mixed derivative on $\partial^2 f_i'/\partial m_i' \partial r_i'$, telling whether the benefit of the mating trait investment r_i increases or decreases with gamete size m_i, follows the same sign as for $\partial f_i'/\partial m_i'$, and tells whether the trait is more efficient for smaller or larger gametes, and if anisogamy evolves, we can indeed see that this mixed derivative predicts in most cases which mating type invests more into the mating trait.

S2.5 Our model in terms of Lehtonen et al 2016 fitness formulation.

S2.5.1 The fitness formulation of Lehtonen et al. In Lehtonen et al. (2016), when analysing the expanded model, absolute fitness (to which we refer to as reproductive success F_i) is divided up into three fitness components,

$$F_i = S_i c_i G, \tag{S17}$$

where S_i is the probability of an individual to find a mating pool (in our model we assume $S_i = 1$), G is group-level fecundity (the mating pool's total number of successful fertilizations) and c_i is the gamete competition function, giving the proportion of the group-level fecundity resulting from focal fertilizations.

In Lehtonen et al. (2016) a gamete competition function c_i is assumed, where individuals can only compete thorough gamete numbers, and the fitness component c_i is therefore unable to generate asymmetries between the sexes (Lehtonen et al. (2016) S2). The authors also point out that the same holds for the mate searching function S_i, and only group-level fecundity G is investigated as a candidate to generate sex-differential selection. However, for our model G has no effect on selection (see next subsection), while the gamete competition function c_i is alone responsible for the sex-differential selection leading to female- or male-biased competition.

S2.5.2 Invasion fitness in a large group. In this subsection, we show that the evolutionary dynamics of our model is only dependent on the fitness component of the competition function c_i, which is therefore the fitness component responsible for the sex-differential selection in our model.

By rewriting equation S17, we find that this gamete competition function is given by

$$c_i = F_i/G, \tag{S18}$$

assuming $S_i = 1$ (which the authors also do when investigating the gamete competition function). For a mating pool with a group size k and with only the resident strategy we get $G = kF_i$, while if a focal mutant individual is present it is given by $G' = (k-1)F_i + F_i')$.

For a mutant individual, equation S18 equals $c_i = F_i'/[(k-1)F_i + F_i']$. In our model, we assume large population size, but also implicitly large group size k, such that no group effects are needed to be considered. Large k gives $G' = G$ (i.e., the effect of a rare mutant on group-level fecundity G' is negligible when the group is large) and therefore $c_i' = F_i'/(kF_i)$. Mutant absolute fitness F_i' over population mean fitness F_i equals mutant relative fitness w_i. Therefore, the gamete competition function equals $c_i = w_i'/k$ and we get that $w_i' = kc_i'$ (note that for a resident strategy, we always have $c_i = 1/k$ and $w_i = 1$).

In conclusion, assuming large population and large groups, the invasion fitness of a rare mutant strategy T' (Shaw and Mohler equation, equation 4) simplifies to,

$$w(T', T) = k\frac{\left(c_x'(m_x', r_x', T) + c_y'(m_y', r_y', , T)\right)}{2}. \tag{S19}$$

This is simply the group size k times the expected proportion of the group's fitness being focal. Thereby, our result is only dependent on the gamete competition function c_i.

S2.6 Intrasexual cost and intersexual benefit of the mating trait. We assess the competitive nature of a mating trait by measuring its intrasexual cost. The intrasexual cost represents the relative reduction in reproductive success experienced by a focal individual (as defined in Eq. A14) when there is an increase in the mating trait investment of other individuals of the same mating type.

In our model, the mating trait can only be produced by allocating a certain proportion r_i of the energy budget to it, thereby reducing the number of gametes produced (as described in Eq. 1). However, in this context, our aim is to examine the effect of the mating trait on a focal individual when other individuals increase the trait, without considering the cost of this trait to the individuals increasing it. To accomplish this, we introduce the term u_i, which represents the unconstrained investment in the mating trait. This term is added to the mating trait investment r_i of the other individuals of the same mating type (in Eq.2 for the motility trait or Eq.3 for the fusion partner capture trait). Notably, the introduction of u_i does not reduce the number of gametes produced (in Eq. 1), i.e., it increases the investment in the mating trait without any trade-off. In this specific context, the strategy is given by T_u having this extra trait: $T_u = (m_x, r_x, u_x, m_y, r_y, u_y)$. Hence, the intrasexual cost is given by the relative decrease in reproductive success of a focal individual F_i', as other individuals increases their unconstrained investment of the mating trait,

$$-\left(\frac{1}{F_i'(T_u', T_u)}\frac{\partial F_i'(T_u', T_u)}{\partial u_i}\Big|_{u_i=u_j=0}\right)\Big|_{T_u'=T_u}, \qquad [S20]$$

where i denotes the mating type of the focal individual, and the minus ensures that the intrasexual cost measures a decrease, rather than an increase in reproductive success.

We also quantify the intersexual benefit of the mating trait, which is the relative increase in reproductive success experienced by a focal individual when the mating trait of the individuals of the opposite mating type in the population is increased. This benefit is measured by

$$\left(\frac{1}{F_i'(T_u', T_u)}\frac{\partial F_i'(T_u', T_u)}{\partial u_j}\Big|_{u_i=u_j=0}\right)\Big|_{T_u'=T_u}, \qquad [S21]$$

We note that the intrasexual cost and intersexual benefit of the mating trait do not indicate selection directly acting on the trait, since the fitness effect is not measured on the individuals carrying the trait.

S3. Step-wise calculations.

S3.1 Solving for gamete fertilization. In the mating pool, the number of gametes per zygote of mating type i at time t decreases as fertilization events occur according to (Eq. A5)

$$\frac{\mathrm{d}n_{i,t}}{\mathrm{d}t} = -c_r n_{i,t}(n_{i,t} + n_{j,0} - n_{i,0}),$$

which is a separable differential equation:

$$\begin{aligned} \frac{\mathrm{d}n_{i,t}}{\mathrm{d}t} &= -c_r n_{i,t}^2 - c_r(n_{j,0} - n_{i,0})n_{i,t} \quad \Longleftrightarrow \\ \frac{\frac{\mathrm{d}n_{i,t}}{\mathrm{d}t}}{c_r n_{i,t}^2 + c_r(n_{j,0} - n_{i,0})n_{i,t}} &= -1, \end{aligned}$$

and can thereby be solved by integrating both sides with respect to t using the definite integral from $t = 0$ to $t = \tau$

$$\begin{aligned} \int_0^\tau \frac{\frac{\mathrm{d}n_{i,t}}{\mathrm{d}t}}{c_r n_{i,t}^2 + c_r(n_{j,0} - n_{i,0})n_{i,t}}\mathrm{d}t &= -\int_0^\tau 1 \ \mathrm{d}t \quad \Longleftrightarrow \\ \int_{n_{i,0}}^{n_{i,\tau}} \frac{1}{(c_r + \frac{c_r(n_{j,0}-n_{i,0})}{n_{i,t}})n_{i,t}^2}\mathrm{d}n_{i,t} &= -\tau \end{aligned}$$

The left-hand side integral can be solved with the following substitution $u(n_{i,t}) = c_r + c_r(n_{j,0} - n_{i,0})/n_{i,t}$ and $\mathrm{d}u = -c_r(n_{j,0} - n_{i,0})/n_{i,t}^2 \mathrm{d}n_{i,t} \iff \mathrm{d}n_{i,t} = -n_{i,t}^2/(c_r(n_{j,0} - n_{i,0}))\mathrm{d}u$, resulting in

$$\begin{aligned} -\frac{1}{c_r(n_{j,0} - n_{i,0})}\int_{u(n_{i,0})}^{u(n_{i,\tau})} \frac{1}{u}\mathrm{d}u &= -\tau \quad \Longleftrightarrow \\ \frac{1}{c_r(n_{j,0} - n_{i,0})}\left[\log(u)\right]_{u(n_{i,0})}^{u(n_{i,\tau})} &= \tau \quad \Longleftrightarrow \\ \frac{\log\left(u\left(n_{i,\tau}\right)/u\left(n_{i,0}\right)\right)}{c_r(n_{j,0} - n_{i,0})} &= \tau. \end{aligned}$$

Substituting back $u(n_{i,t}) = c_r + c_r(n_{j,0} - n_{i,0})/n_{i,t}$ gives

$$\begin{aligned} \log\left(\frac{1 + (n_{j,0} - n_{i,0})/n_{i,\tau}}{1 + (n_{j,0} - n_{i,0})/n_{i,0}}\right) &= c_r(n_{j,0} - n_{i,0})\tau \quad \Longleftrightarrow \\ \frac{n_{i,0} + n_{i,0}(n_{j,0} - n_{i,0})/n_{i,\tau}}{n_{j,0}} &= \exp\Big(c_r(n_{j,0} - n_{i,0})\tau\Big) \quad \Longleftrightarrow \\ n_{i,\tau} &= \frac{n_{i,0}(n_{j,0} - n_{i,0})}{\exp\Big(c_r(n_{j,0} - n_{i,0})\tau\Big)n_{j,0} - n_{i,0}} \end{aligned}$$

Substituting τ with t gives the explicit expression for the number of gametes of mating type i at time t

$$n_{i,t} = \frac{n_{i,0}(n_{j,0} - n_{i,0})}{\exp\Big(c_r(n_{j,0} - n_{i,0})t\Big)n_{j,0} - n_{i,0}}. \qquad [S22]$$

S3.2 Solving for gamete fertilization under isogamy. For the case of the isogamic constraint, the number of gametes per zygote of mating type i at time t decreases according to (Eq. A7)

$$\frac{\mathrm{d}n_{i,t}}{\mathrm{d}t} = -c_r n_{i,t}^2,$$

which is a separable differential equation:

$$\begin{aligned} \frac{\mathrm{d}n_{i,t}}{\mathrm{d}t} &= -\,c_r n_{i,t}^2 \quad \Longleftrightarrow \\ \frac{\frac{\mathrm{d}n_{i,t}}{\mathrm{d}t}}{n_{i,t}^2} &= -\,c_r, \end{aligned}$$

and can thereby be solved by integrating both sides with respect to t using the definite integral from $t = 0$ to $t = \tau$

$$\begin{aligned} \int_0^\tau \frac{\frac{\mathrm{d}n_{i,t}}{\mathrm{d}t}}{n_{i,t}^2}\mathrm{d}t &= -\int_0^\tau c_r\ \mathrm{d}t \quad \Longleftrightarrow \\ \int_{n_{i,0}}^{n_{i,\tau}} \frac{1}{n_{i,t}^2}\mathrm{d}n_{i,t} &= -\,c_r\tau \quad \Longleftrightarrow \\ \left[\frac{1}{n_{i,t}}\right]_{n_{i,0}}^{n_{i,\tau}} &= c_r\tau \quad \Longleftrightarrow \\ \frac{1}{n_{i,\tau}} &= c_r\tau + \frac{1}{n_{i,0}} \quad \Longleftrightarrow \\ \frac{1}{n_{i,\tau}} &= \frac{c_r n_{i,0}\tau + 1}{n_{i,0}} \quad \Longleftrightarrow \\ n_{i,\tau} &= \frac{n_{i,0}}{c_r n_{i,0}\tau + 1} \end{aligned}$$

Substituting τ with t gives the explicit expression for the number of gametes of mating type i at time t under isogamy

$$n_{i,t} = \frac{n_{i,0}}{c_r n_{i,0} t + 1}. \qquad [S23]$$

S3.3 Solving for gamete fertilization of a rare mutant strategy. In the mating pool, the number of gametes per zygote with a rare mutant strategy, of mating type i at time t, decreases according to (Eq. A12)

$$\frac{\mathrm{d}n_{i',t}}{\mathrm{d}t} = -\frac{c_m n_{j,0}(n_{i,0}-n_{j,0})}{\exp\big(c_r(n_{i,0}-n_{j,0})t\big)n_{i,0}-n_{j,0}}n_{i',t},$$

which is a separable differential equation

$$\begin{aligned}\frac{\mathrm{d}n_{i',t}}{\mathrm{d}t} &= -\frac{c_m(n_{i,0}-n_{j,0})n_{j,0}}{\exp(c_r(n_{i,0}-n_{j,0})t)n_{i,0}-n_{j,0}}n_{i',t} \quad \iff \\ \frac{\frac{\mathrm{d}n_{i',t}}{\mathrm{d}t}}{n_{i',t}} &= -\frac{c_m(n_{i,0}-n_{j,0})n_{j,0}}{\exp(c_r(n_{i,0}-n_{j,0})t)n_{i,0}-n_{j,0}},\end{aligned}$$

and can thereby be solved by integrating both sides with respect to t using the definite integral from $t=0$ to $t=\tau$

$$\begin{aligned}\int_0^\tau \frac{\frac{\mathrm{d}n_{i',t}}{\mathrm{d}t}}{n_{i',t}}\mathrm{d}t &= -\int_0^\tau \frac{c_m(n_{i,0}-n_{j,0})n_{j,0}}{\exp(c_r(n_{i,0}-n_{j,0})t)n_{i,0}-n_{j,0}}\mathrm{d}t \quad \iff \\ \int_{n_{i,0}}^{n_{i,\tau}} \frac{1}{n_{i',t}}\mathrm{d}n_{i',t} &= -c_m(n_{i,0}-n_{j,0})n_{j,0}\int_0^\tau \frac{1}{\exp(c_r(n_{i,0}-n_{j,0})t)n_{i,0}-n_{j,0}}\mathrm{d}t \iff \\ \Big[\log(n_{i',t})\Big]_{n_{i',0}}^{n_{i,\tau}} = \log\left(\frac{n_{i',t}}{n_{i',0}}\right) &= -c_m(n_{i,0}-n_{j,0})n_{j,0}\int_0^\tau \frac{1}{\exp(c_r(n_{i,0}-n_{j,0})t)n_{i,0}-n_{j,0}}\mathrm{d}t\end{aligned}$$

The right hand side integral can be solved by first applying the following substitution $u(t) = c_r(n_{i,0}-n_{j,0})t$ where $\mathrm{d}u = c_r(n_{i,0}-n_{j,0})\mathrm{d}t \iff \mathrm{d}t = 1/c_r(n_{i,0}-n_{j,0})\mathrm{d}u$, resulting in

$$\begin{aligned}\log\left(\frac{n_{i',t}}{n_{i',0}}\right) &= -\frac{c_m(n_{i,0}-n_{j,0})n_{j,0}}{c_r(n_{i,0}-n_{j,0})}\int_{u(0)}^{u(\tau)}\frac{1}{\exp(u)n_{i,0}-n_{j,0}}\mathrm{d}u \quad \iff \\ \log\left(\frac{n_{i',t}}{n_{i',0}}\right) &= -\frac{c_m n_{j,0}}{c_r}\int_0^\tau \frac{1}{\exp(u)n_{i,0}-n_{j,0}}\mathrm{d}u,\end{aligned}$$

and then apply the following substitution $v(u) = \exp(u)$ where $\mathrm{d}v = \exp(u)\mathrm{d}u \iff \mathrm{d}u = (1/v)\mathrm{d}v$, resulting in

$$\log\left(\frac{n_{i',t}}{n_{i',0}}\right) = -\frac{c_m n_{j,0}}{c_r}\int_{v[u(0)]}^{v[u(\tau)]}\frac{1}{v(n_{i,0}v-n_{j,0})}\mathrm{d}v, \tag{S24}$$

and the right-hand side can be simplified using partial fraction decomposition:

$$\begin{aligned}\frac{1}{v(n_{i,0}v-n_{j,0})} &= \frac{A}{v}+\frac{B}{n_{i,0}v-n_{j,0}} \quad \iff \\ 1 &= A(n_{i,0}v-n_{j,0})+Bv\end{aligned}$$

where $v = n_{j,0}/n_{i,0}$ gives the solution $B = n_{i,0}/n_{j,0}$, and $v=0$ gives the solution $A = -1/n_{j,0}$. Hence,

$$\frac{1}{v(n_{i,0}v-n_{j,0})} = \frac{n_{i,0}}{n_{i,0}n_{j,0}v-n_{j,0}^2}-\frac{1}{n_{j,0}v} \tag{S25}$$

Substituting Eq. S25 into Eq. S24 gives

$$\log\left(\frac{n_{i',t}}{n_{i',0}}\right) = -\frac{c_m n_{j,0}}{c_r}\left(-\int_{v[u(0)]}^{v[u(\tau)]}\frac{1}{n_{j,0}v}\mathrm{d}v + \int_{v[u(0)]}^{v[u(\tau)]}\frac{n_{i,0}}{n_{i,0}n_{j,0}v - n_{j,0}^2}\mathrm{d}v\right) \iff$$

$$\log\left(\frac{n_{i',t}}{n_{i',0}}\right) = \frac{c_m}{c_r}\int_{v[u(0)]}^{v[u(\tau)]}\frac{1}{v}\mathrm{d}v \quad - \quad \frac{c_m n_{i,0}}{c_r}\int_{v[u(0)]}^{v[u(\tau)]}\frac{1}{n_{i,0}v - n_{j,0}}\mathrm{d}v, \qquad \text{[S26]}$$

Solving for the integral on the left in Eq. S26 and then substituting back $v = \exp(u)$, and then $u = c_r(n_{i,0} - n_{j,0})t$ gives

$$\begin{aligned}\int_{v[u(0)]}^{v[u(\tau)]}\frac{1}{v}\mathrm{d}v &= \Big[\log(v)\Big]_{v[u(0)]}^{v[u(\tau)]}\\ &= \log\Big(v\big(u(\tau)\big)\Big) - \log\Big(v\big(u(0)\big)\Big)\\ &= u(\tau) - u(0)\\ &= c_r(n_{i,0} - n_{j,0})\tau \end{aligned} \qquad \text{[S27]}$$

The integral on the right in Eq. S26 can be solved with the following substitution $w(v) = n_{i,0}v - n_{j,0}$ where $\mathrm{d}w = n_{i,0}\mathrm{d}v \iff \mathrm{d}v = 1/n_{i,0}\mathrm{d}w$, resulting in

$$\begin{aligned}\int_{v[u(0)]}^{v[u(\tau)]}\frac{1}{n_{i,0}v - n_{j,0}}\mathrm{d}v &= \frac{1}{n_{i,0}}\int_{w(v[u(0)])}^{w(v[u(\tau)])}\frac{1}{w}\mathrm{d}w\\ &= \frac{1}{n_{i,0}}\Big[\log(w)\Big]_{w(v[u(0)])}^{w(v[u(\tau)])}\\ &= \frac{1}{n_{i,0}}\log\Big(w\Big(v\big(u(\tau)\big)\Big)\Big) - \log\Big(w\Big(v\big(u(0)\big)\Big)\Big)\\ &= \frac{1}{n_{i,0}}\log\left(\frac{w\Big(v\big(u(\tau)\big)\Big)}{w\Big(v\big(u(0)\big)\Big)}\right)\end{aligned}$$

Substituting back $w = n_{i,0}v - n_{j,0}$, and then $v = \exp(u)$, and then $u = c_r(n_{i,0} - n_{j,0})t$ gives

$$\begin{aligned}&= \frac{1}{n_{i,0}}\log\left(\frac{w\Big(v\big(u(\tau)\big)\Big)}{w\Big(v\big(u(0)\big)\Big)}\right)\\ &= \frac{1}{n_{i,0}}\log\left(\frac{\exp\big(u(\tau)\big)n_{i,0} - n_{j,0}}{\exp\big(u(0)\big)n_{i,0} - n_{j,0}}\right)\\ &= \frac{1}{n_{i,0}}\log\left(\frac{\exp\big(c_r(n_{i,0} - n_{j,0})\tau\big)n_{i,0} - n_{j,0}}{n_{i,0} - n_{j,0}}\right)\end{aligned} \qquad \text{[S28]}$$

Substituting the left and the right integral in Eq. S26 with Eqs. S27 and S28, respectively, gives

$$\begin{aligned}
\log\left(\frac{n_{i',t}}{n_{i',0}}\right) =& c_m(n_{i,0}-n_{j,0})\tau \quad - \quad \frac{c_m}{c_r}\log\left(\frac{\exp\big(c_r(n_{i,0}-n_{j,0})\tau\big)n_{i,0}-n_{j,0}}{n_{i,0}-n_{j,0}}\right) \quad \Longleftrightarrow \\
\log\left(\frac{n_{i',t}}{n_{i',0}}\right) =& c_m(n_{i,0}-n_{j,0})\tau \quad + \quad \frac{c_m}{c_r}\log\left(\frac{n_{i,0}-n_{j,0}}{\exp\big(c_r(n_{i,0}-n_{j,0})\tau\big)n_{i,0}-n_{j,0}}\right) \quad \Longleftrightarrow \\
\frac{n_{i',t}}{n_{i',0}} =& \frac{\exp(c_m n_{i,0}\tau)}{\exp(c_m n_{j,0}\tau)}\left(\frac{\exp(c_r n_{j,0}\tau)(n_{i,0}-n_{j,0})}{\exp(c_r n_{i,0}\tau)n_{i,0}-\exp(c_r n_{j,0}\tau)n_{j,0}}\right)^{\frac{c_m}{c_r}} \quad \Longleftrightarrow \\
\frac{n_{i',t}}{n_{i',0}} =& \frac{\exp(c_m n_{i,0}\tau)}{\exp(c_r n_{j,0}\tau)^{\frac{c_m}{c_r}}}\left(\frac{\exp(c_r n_{j,0}\tau)(n_{i,0}-n_{j,0})}{\exp(c_r n_{i,0}\tau)n_{i,0}-\exp(c_r n_{j,0}\tau)n_{j,0}}\right)^{\frac{c_m}{c_r}} \quad \Longleftrightarrow \\
n_{i',t} =& n_{i',0}\exp(c_m n_{i,0}\tau)\left(\frac{n_{i,0}-n_{j,0}}{\exp(c_r n_{i,0}\tau)n_{i,0}-\exp(c_r n_{j,0}\tau)n_{j,0}}\right)^{\frac{c_m}{c_r}} \quad \Longleftrightarrow
\end{aligned}$$

Substituting τ with t gives the explicit expression for the number of gametes of the mutant strategy of mating type i at time t

$$n_{i',t} = n_{i',0}\exp(c_m n_{i,0}t)\left(\frac{n_{i,0}-n_{j,0}}{n_{i,0}\exp(c_r n_{i,0}t)-n_{j,0}\exp(c_r n_{j,0}t)}\right)^{\frac{c_m}{c_r}} \qquad [S29]$$

S3.4 Solving for gamete fertilization of a rare mutant strategy under isogamy. For the case of the isogamic constraint, the number of gametes per zygote of mating type i with a rare mutant strategy at time t decreases according to (Eq. A12)

$$\frac{\mathrm{d}n_{i',t}}{\mathrm{d}t} = -\frac{c_m n_{i,0}}{c_r n_{i,0} t + 1} n_{i',t},$$

which is a separable differential equation

$$\begin{aligned} \frac{\mathrm{d}n_{i',t}}{\mathrm{d}t} &= -\frac{c_m n_{i,0}}{c_r n_{i,0} t + 1} n_{i',t} \quad \iff \\ \frac{\frac{\mathrm{d}n_{i',t}}{\mathrm{d}t}}{n_{i',t}} &= -\frac{c_m n_{i,0}}{c_r n_{i,0} t + 1} \end{aligned}$$

and can thereby be solved by integrating both sides with respect of t using the definite integral from $t = 0$ to $t = \tau$

$$\begin{aligned} \int_0^\tau \frac{\frac{\mathrm{d}n_{i',t}}{\mathrm{d}t}}{n_{i',t}} \mathrm{d}t &= -\int_0^\tau \frac{c_m n_{i,0}}{c_r n_{i,0} t + 1} \mathrm{d}t \quad \iff \\ \int_{n_{i,0}}^{n_{i,\tau}} \frac{1}{n_{i',t}} \mathrm{d}n_{i',t} &= -c_m n_{i,0} \int_0^\tau \frac{1}{c_r n_{i,0} t + 1} \mathrm{d}t \quad \iff \\ \log\left(\frac{n_{i',t}}{n_{i',0}}\right) &= -c_m n_{i,0} \int_0^\tau \frac{1}{c_r n_{i,0} t + 1} \mathrm{d}t. \end{aligned}$$

The right hand-side of the integral can be solved with the following substitution $u(t) = c_r n_{i,0} t + 1$ where $\mathrm{d}u = c_r n_{i,0} \mathrm{d}t \iff \mathrm{d}t = 1/(c_r n_{i,0}) \mathrm{d}u$, resulting in

$$\begin{aligned} \log\left(\frac{n_{i',t}}{n_{i',0}}\right) &= -\frac{c_m n_{i,0}}{c_r n_{i,0}} \int_{u(0)}^{u(\tau)} \frac{1}{u} \mathrm{d}u \quad \iff \\ \log\left(\frac{n_{i',t}}{n_{i',0}}\right) &= -\frac{c_m}{c_r} \log\left(\frac{u(0)}{u(\tau)}\right) \quad \iff \\ n_{i',t} &= n_{i',0} \left(\frac{u(\tau)}{u(0)}\right)^{\frac{c_m}{c_r}}. \end{aligned}$$

Substituting back $u(v) = c_r n_{i,0} t + 1$ and then τ with t gives the explicit expression for the number of gametes of the mutant strategy of mating type i at time t under isogamy

$$n_{i',t} = n_{i',0} \frac{1}{(c_r n_{i,0} t + 1)^{\frac{c_m}{c_r}}}. \qquad [S30]$$

S4. Supplementary figures

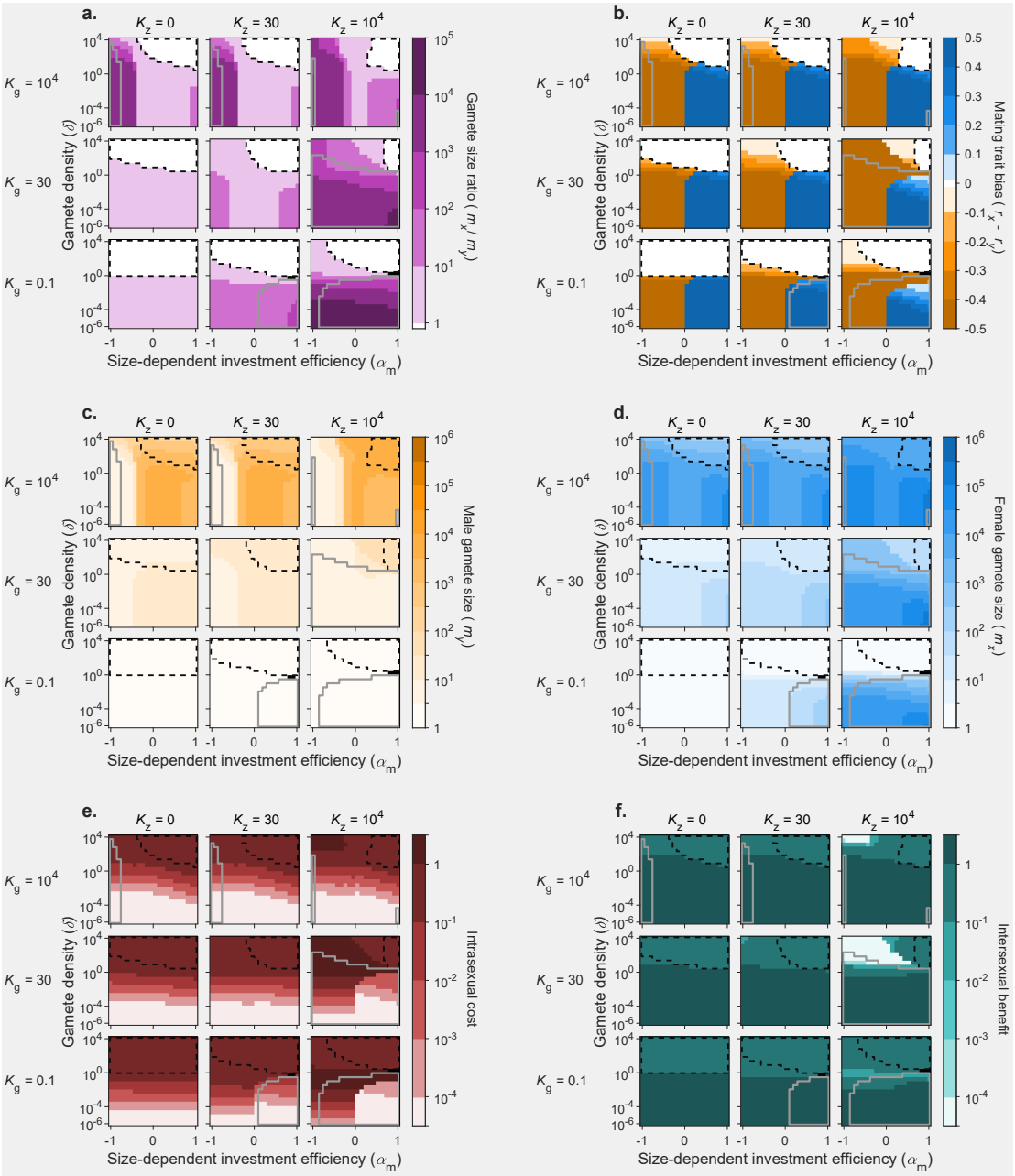

Fig. S1. Sexual dimorphism in gamete size (**a.**) and sex-bias in mating trait investment between the two mating types x and y (**b.**), male and female gamete size (**c.** and **d.**, respectively), intrasexual cost (**e.**) and intersexual benefit (**f.**) of the mating trait, for the case of motility. The vertical axis of each subplot represents the gamete density constant δ and the horizontal axis of each subplot represents the size-dependent investment efficiency α_m, which modulates whether gamete size has a positive or negative effect on the efficiency of energy invested into motility. We present results for three values of K_z, the size-dependent survival parameter for zygotes, and for three values of K_g, the size-dependent survival parameter for gametes. Contour lines correspond to derivations of the stability analysis. A black dashed line encapsulates the area where isogamy is the expected evolutionary end-point; in the remaining area, anisogamy is expected. A grey contour line encapsulates the area where a pseudo-isogamic genetic polymorphism can occur before anisogamy evolves. The results from solving the evolutionary path are represented by the coloured shading showing the degree of sexual dimorphism in gamete size (**a.**) and investment in the mating trait (**b.**) reached at the evolutionary endpoint, where white represents no dimorphism, and deep colours represent strong dimorphism. Note that under anisogamy, it is always only one mating type that invests into the mating trait. The gamete sizes for the male and female mating types are given in **c.** and **d.**, respectively. The intrasexual cost (and intersexual benefit) of the mating trait is given in **e.** (and **f.**), measured as the relative decrease (increase) in reproductive success of a focal individual (Eq. A14) as the result of increasing the mating trait investment of other same-mating type (opposite mating type) individuals (details are given in Supplementary information S2.6). For anisogamic parameter region, the intrasexual cost (intersexual benefit) is evaluated for the mating type that invests (do not invest) into the mating trait.

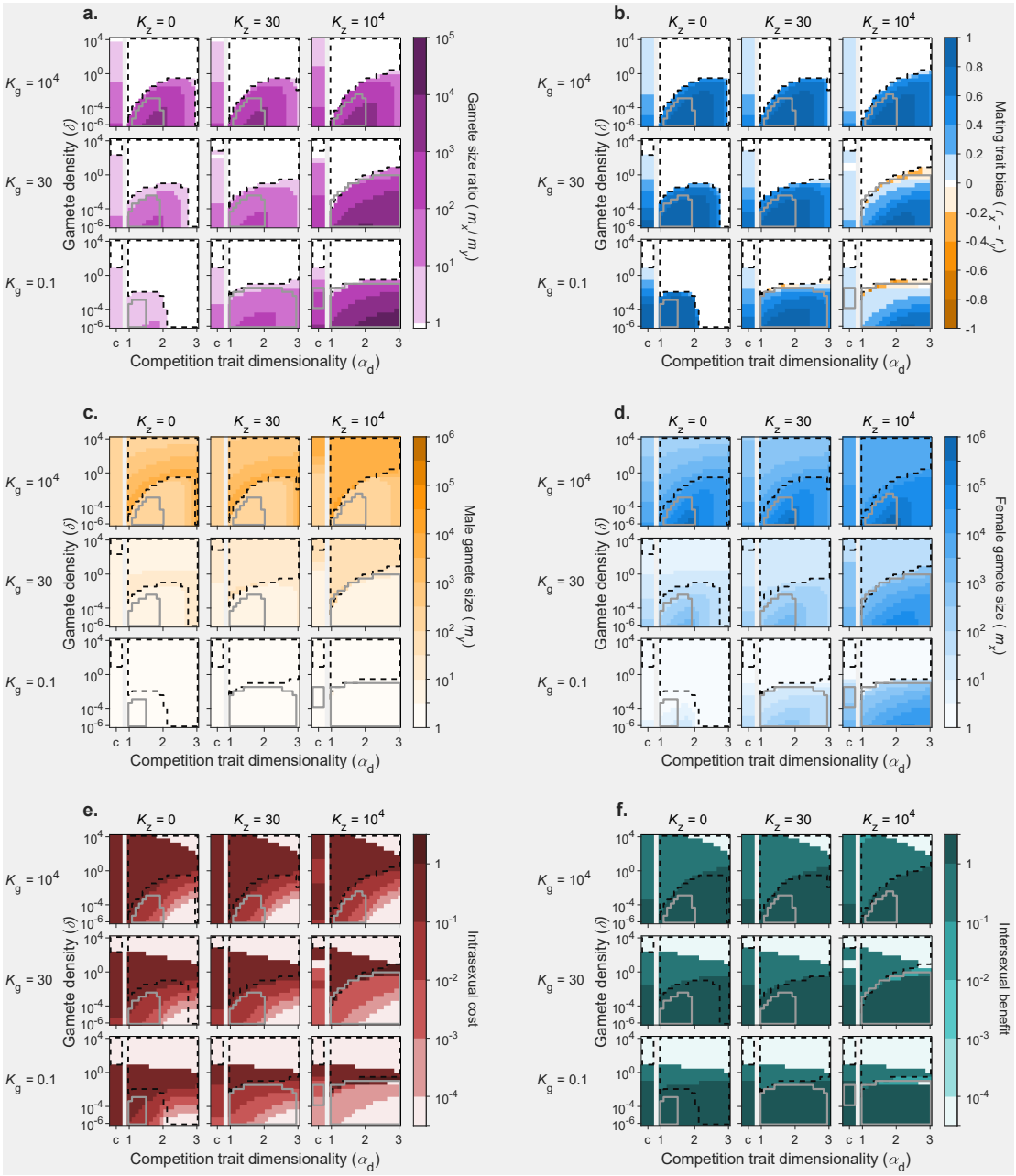

Fig. S2. Sexual dimorphism in gamete size (**a.**) and sex-bias in mating trait investment between the two mating types x and y (**b.**), male and female gamete size (**c.** and **d.**, respectively), intrasexual cost (**e.**) and intersexual benefit (**f.**) of the mating trait, for the case of fusion partner capture. The vertical axis of each subplot represents the gamete density constant δ and the horizontal axis of each subplot represents the dimensionality parameter α_d ranging from 1 to 3, which determines how costly the physical structures are (low α_d means low cost). The left part of each plot is reserved for the special case of chemoattraction, denoted by a c on the plot axis and separated by a gray bar from the physical structure case. We present results for three values of K_z, the size-dependent survival parameter for zygotes, and for three values of K_g, the size-dependent survival parameter for gametes. Contour lines correspond to derivations of the stability analysis. A black dashed line encapsulates the area where isogamy is the expected evolutionary end-point; in the remaining area, anisogamy is expected. A grey contour line encapsulates the area where a pseudo-isogamic genetic polymorphism can occur before anisogamy evolves. The results from solving the evolutionary path are represented by the coloured shading showing the degree of sexual dimorphism in gamete size (**a.**) and investment bias in the mating trait (**b.**) reached at the evolutionary endpoint, where white represents no dimorphism, and deep colours represent strong dimorphism. Note that under anisogamy, it is almost always only one mating type that invests into the mating trait. The gamete sizes for the male and female mating types are given in **c.** and **d.**, respectively. The intrasexual cost (and intersexual benefit) of the mating trait is given in **e.** (and **f.**), measured as the relative decrease (increase) in reproductive success of a focal individual (Eq. A14) as the result of increasing the mating trait investment of other same-mating type (opposite mating type) individuals (details are given in Supplementary information S2.6). For anisogamic parameter region, the intrasexual cost (intersexual benefit) is evaluated for the mating type investing more (less) into the mating trait. Note: for $K_z = 10^4$ and $K_g = 0.1$ and 30, the grey contour line encapsulates one pixel (one parameter combination) in the isogamic region. Genetic polymorphism in the isogamic region could be an error due to numerical imprecision, or potentially show that a fourth evolutionary outcome is possible for a very restrictive parameter space, where only genetic polymorphism can evolve.